Application Guide on the Use of MTG LI in Severe Convective Storms Nowcasting

Disclaimer:

Please note that, at the time of writing, knowledge on LI data interpretation in severe storms is still limited due to the small number of cases available for analysis.

This guide is intended as a compact training basis for the ESSL-EUMETSAT Forecaster Testbeds and other training events at ESSL, EUMETSAT and national weather services and does not replace official EUMETSAT documents.

For updated and legally binding materials, please refer to the latest version of the EUMETSAT User Portal: https://user.eumetsat.int/resources/user-guides/using-mtg-lightning-imager-li-to-track-convective-storms

 (ESSL Report 2025-01)

How to cite:
Holzer, A. M., et. al.: EUMETSAT-ESSL Application Guide on the Use of MTG LI in Severe Convective Storms Nowcasting, ESSL Report 2025-01, https://www.essl.org/cms/essl-testbed, 2025.

Application Guide on the Use of MTG LI in Severe Convective Storms Nowcasting

Version 3.1.4 – 7 March 2025

Alois M. Holzer

- affiliated with the European Severe Storms Laboratory, ESSL -

and contributors (see Addendum for full name list)

Content

Chapter 1: Understanding lightning data

Basics about lightning and its detection

Every lightning flash requires a sequence of processes that can be summarized[1] as follows:

A flash initiates typically deep within the cloud, where the electric field exceeds the breakdown threshold. This happens between regions or layers of oppositely charged cloud/precipitation particles.

Shortly after initiation, a conductive hot channel forms, called leader, which is polarized and grows bi-directionally. The positive leader branches out into layers of negatively charged particles, while the negative leader branches into layers of positive particles. The negative leader propagates with steps on the order of 10-100 microseconds (μs) and 10-100 meters. The leaders grow until the field at their tips becomes insufficient. In the later stages of the flash, parts of previously formed lightning channels cool down, becoming resistive and cut off, which gives rise to secondary processes, which have been given many names, such as needles, recoil leaders and K-changes. These fast processes of various sizes tend to be more impulsive and repetitive.

A leader branch can propagate out of the cloud and connect to ground (a cloud-to-ground flash). This is followed by a return stroke of great intensity and may be followed by multiple strokes through the same channel, usually separated by tens or hundreds of milliseconds (ms), or grow new branches to ground in other locations. The subsequent strokes are caused by downward dart leaders initiated from the part of the flash rooted inside the cloud. Lightning flashes may initiate at tall objects on the ground. Some flashes can branch out into the stratiform precipitation region under the anvil canopy of mesoscale convective systems, growing tens to hundreds of kilometers wide. These usually also produce cloud-to-ground strokes in various locations.

Definitions of key terminology with relevance to LI data inter

The following glossary is provided for reference and was kindly compiled by Oscar van der Velde. It is built on further reading by Rakov & Uman (2003), NWS (2024), AMS (2024), and Fdez-Arroyabe, Kourtidis, Haldoupis, & al. (2021).

Lightning

Collective name for any electric discharges in a planetary atmosphere which involve hot leader channels.

Flash

An event of lightning, detectable as a burst of optical and electromagnetic energy: the complete sequence of processes following electric breakdown, from initial formation of channels to the last sign of electrical activity, including any strokes (be it intracloud or cloud-to-ground). Flashes are separated by periods without detectable processes.

Return stroke or stroke

Intense current between cloud and ground, following the connection of a leader with ground. Strokes are detectable by their impulsive emissions in the very low frequency range of the electromagnetic spectrum. Strokes, from the perspective of lightning detection networks, include impulsive lightning processes inside the cloud (usually at the beginning of flashes) such as narrow bipolar events (NBE) or energetic in-cloud pulses (EIP).

Discharge

In general, a collective name for any electric discharge, including lightning, sparks, and cold discharges in the form of corona and streamers (e.g. including Saint Elmo's Fire, sprites and blue jets).

[1] Lightning terminology kindly provided by Oscar van der Velde (2024), UPC.

Intracloud discharge or flash

Lightning flash that only involves in-cloud lightning processes, without connecting to the ground. If a polarity is indicated, it indicates the dipole polarity (e.g. +IC is a discharge between positive charge region over a negative charge region).

Cloud-to-ground discharge or flash

Lightning flash that includes a return stroke connecting cloud and ground. Its polarity indicates the charge removed from the cloud.

Upward lightning

Lightning flash initiated at a ground-based object, connecting to the cloud.

Bolt-from-the-blue

Negative cloud-to-ground flash (-CG stroke) in which the negative leader first grows upward and escapes from the side of the convective cloud. Among storm chasers, it is often incorrectly claimed to be a "positive bolt" because they believe it is a strike from the positively charged top of the thundercloud.

Leader

A hot channel in a lightning discharge or large spark. Usually forms branches. Leader tips are the advancing ends of a leader. They are polarized and focal points for streamer corona that develops in the concentrated electric field around the tips. The resulting heating accomplishes the extension of the leader. In the case of negative leaders (also known as stepped leader), a complex step formation process takes place, involving formation of space stems in the streamer zone ahead of the leader tip. Currents will move freely along leader channels as long as they remain conductive (hot).

Dart leader

A process that occurs after the first return stroke in a channel between cloud and ground, in which a new surge of negative charge propagates rapidly from the cloud to ground through the previously formed cloud-to-ground channel, initiating a new return stroke. This surge is initiated by a recoil process, in which new bi-directional breakdown occurs along old positive leader branches, in electric measurements identified as a "k-change", which also happens in intracloud discharges.

Bidirectional leader or bi-leader

Polarized leader channels with opposite polarity branches moving into different parts of the cloud.

Channel

See leader.

Pulse

Pulses can be optical or electromagnetic pulses recorded by a detector.

Lightning Detection

Lightning flashes radiate over a large energetic spectrum, from electromagnetic to acoustic domains (see Fig. 1-1). Different techniques to detect and locate signals related to lightning flashes are applied from ground, air and space platforms, using different spectral ranges:

Lightning mapping arrays (LMAs) can produce the 3-D image of the lightning flash and concentrate on detecting very high-frequency (VHF) radio signals that originate from the leader that initiates and spreads between the charge centers. LMAs operate only on limited scales, with a coverage on the order of 100 km.

Lightning detection networks (LDNs), also called **Lightning Locating Systems (LLSs),** operating on lower frequencies (LF and VLF) on national, continental, or global scales, concentrate on detecting the signals that originate when the lightning channel is short-circuited, i.e. when the "connection" between two charge centers is "successful" and the return stroke forms.

Lightning Imagers (LIs) are based on sensors that detect the emitted optical light pulses. As a lot of charge is carried in the return stroke phase, the channel heats up and illuminates. This is the phase that is most likely to be detected by a LI. The optical light pulse measured by the sensor is usually influenced by cloud-induced extinction (scattering and absorption).

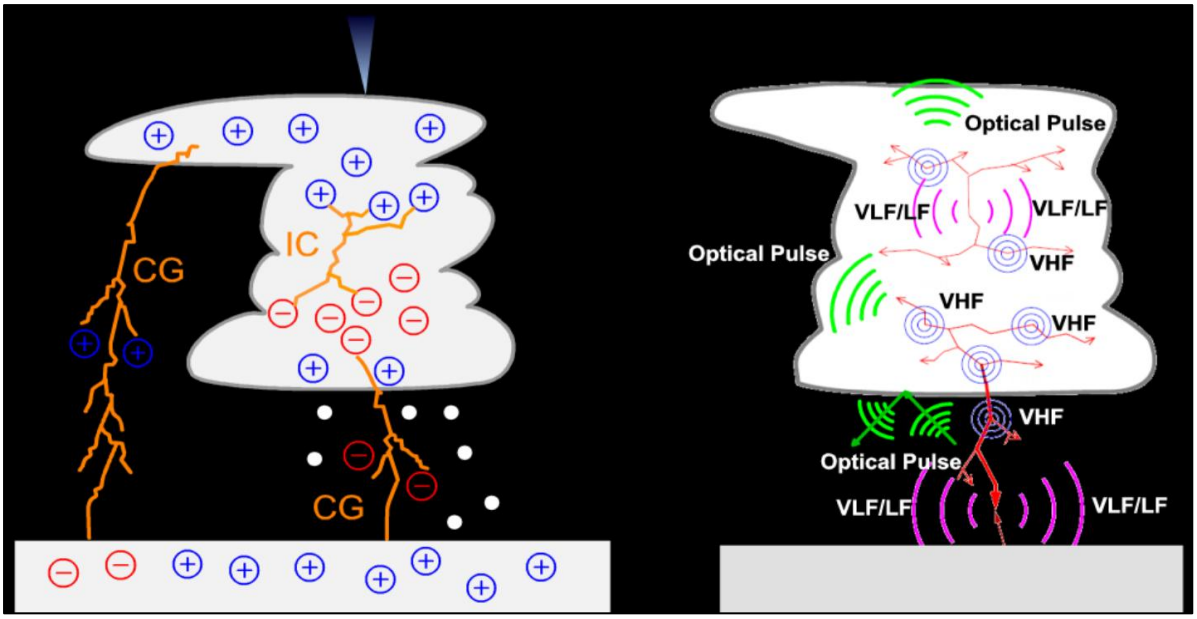

Fig. 1-1: Signals related to lightning discharges. Graphics adapted by Felix Erdmann (Erdmann & Poelman, GLM lightning measurements and their potential use for nowcasting, 2023) from EUMETRAIN (2020).

LMAs and other lightning detection networks are used here as comparison with space-based lightning imager data from the MTG LI instrument. To illustrate how a lightning flash can be detected or seen by remote sensing systems, compared to ground-based detection systems, we provide exemplary visualizations of LI and LMA data.

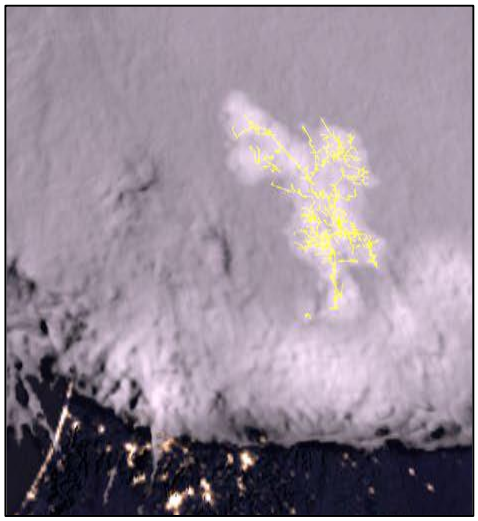

Fig. 1-2: GOES-GLM data overlaid on GeoColor nighttime imagery. Plotting as described in Peterson, Rudlosky, & Deierling (2017) with "eye-candy visualization" optimized for the display of large flashes. Example how LI data could be visualized for outreach and media purposes.

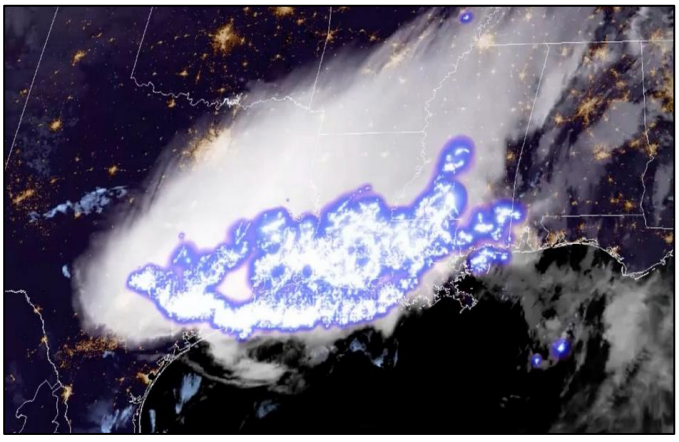

Fig. 1-3: A thunderstorm complex that was found to contain the longest single flash on record within the first years of GOES-GLM data. It covered a horizontal distance of around 768 kilometres (477 miles) across parts of the southern United States on 29 April 2020 (NOAA, 2021) and (NOAA, 2022).

Types of flashes

Within a negative cloud to ground flash (negative CG), negative charge is transported from the cloud to the ground. Within a positive cloud to ground flash (positive CG), positive charge is transported from the cloud to the ground. Negative CGs are more common than positive CGs, given the usual proximity of negative charges at the bottom of a cloud, as illustrated in Fig. 1-5. Within an intra cloud (IC) flash, charge is transported from one part of the cloud to another part of the cloud. The flash process usually lasts a few hundred milliseconds. (López, et al., 2017) found mean lightning lengths of 15 to 18.5 km and median lightning lengths of 10.4 to 15.5 km.

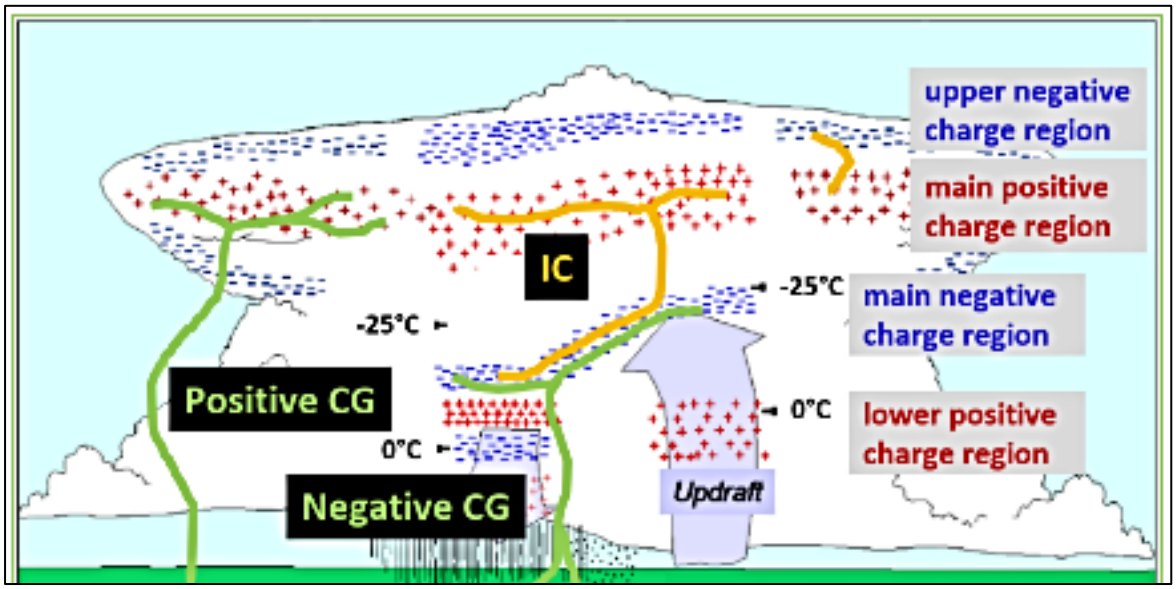

Fig. 1-4: Schematic on CG flashes (with the evolving sequence of bi-leader, ground connection, return stroke, dart leaders and subsequent return strokes) and IC flashes (with bi-leaders and K-changes, i.e. short-term changes of the electric field on the order of milliseconds). (Erdmann & Poelman, 2023) adapted from (Stolzenburg & Marshall, 2009).

A paper by Bruning & MacGorman (2013) describes fundamental thunderstorm properties and their relation to intra-cloud lightning flashes: Charge regions are organized into small pockets in turbulent thunderstorm updrafts. Active and strong updrafts tend to produce short-distance flashes:

> *In and near strong updrafts, flashes tend to be smaller and more frequent, while flashes far from strong vertical drafts exhibit the opposite tendency. This study quantitatively tests these past anecdotal observations using LMA data for two supercell storms that occurred in Oklahoma in 2004. The data support a prediction from electrostatics that frequent breakdown and large flash extents are opposed. … In line with the hypothesized role of convective motions as the generator of thunderstorm electrical energy, the correspondence between kinematic and electrical energy spectra suggests that advection of charge-bearing precipitation by the storm's flow, including in turbulent eddies, couples the electrical and kinematic properties of a thunderstorm.*
>
> *…*
>
> *The examination of local flash statistics for both storms appears to confirm the prediction that average local flash area and local breakdown rate are opposed. The data support an expectation that pixels with a high (low) flash initiation rate would have smaller (larger) average flash sizes.*
>
> (Bruning & MacGorman, 2013)

The phases of a flash and lightning types were most recently described by Erdmann (2020):

Propagating from an initial source, there are four types of leaders that also define four different types of cloud-to-ground (CG) flashes; (i) negative downward, (ii) negative upward, (iii) positive downward, and (iv) positive upward. Anthropogenic constructions such as tall structures, airplanes, and rockets can influence and even trigger **CG flashes**. Negative downward leaders produce **negative CG flashes**.

As illustrated in Figure 1-5 (upper part), they often also have a positive leader that propagates as IC component. This is the most common type of CG flashes. The stepped leader builds several branches seeking for the channel of lowest resistance to connect the cloud and the ground. Negative stepped leaders propagate over several kilometers, despite the fact that there must be a significant E-field to allow for a breakdown ahead of the leader tip. The steps become fainter and propagate slower as the leader approaches the ground. Streamers can emerge from sharp points to facilitate the connection of the leader with the ground. For downward negative leaders, upward positive streamers may attach to the leader tip. Once connected to the ground, the narrow, ionized conducting channel is activated. Negative charge is lowered from the cloud to the ground by an upward return-stroke (Figure 1-5, upper part, step (2)).

The return-stroke moves continuously fast in the opposite direction of the charge transfer. Even after this first, effective discharge, the conducting channel remains active and there is often IC activity (step (3)). Subsequent dart leaders, that move continuously and about two orders of magnitude faster than the stepped leader, can use the existing ionized channel to transfer further charge from the cloud to the ground (step (4)). Hence, dart leaders cause subsequent return-strokes in multi-stroke flashes (step (5)). The entire process is what usually is called a flash. It takes only some milliseconds from the initiation to the return-stroke, and the phases proceed too fast for being captured by the human eye without technical support, e.g., high speed cameras. Even if the phases are of very short duration, a flash can last up to several seconds if leaders merge, separate, or travel long distances.

Similar processes with opposite polarity exist for downward positive leaders (Figure 1-5, lower left) and upward negative leaders. They transport positive charge from the cloud to the ground and produce **positive CG flashes**. Positive CG flash usually consist of the positive downward leader and a negative IC leader as shown in Figure 1-5, lower left, step (1). The return strokes move in opposite direction of the charge transfer upward into the cloud following the ground connection of the positive leader. This flash type is rare for normal polarity thunderstorms, however, the vast majority of CG flashes in inverted polarity storms lower positive charge to the ground.

Cloud flashes are the most frequent flash type. On average, at least two thirds of all lightning remain in the sky, and only one third reaches the ground. Nevertheless, there are less studies on cloud flashes than CG lightning, as the latter directly impacts mankind. Cloud flashes include discharges between the different charge regions inside a cloud or of different clouds, and discharges that start within a cloud and terminate in the clear air. Like for CG flash, an IC flash starts by a bi-leader, i.e., a negative (positive) leader propagating toward the positive (negative) charge region. Figure 1-5 (lower right) illustrates the two main components of an IC flash: (1) a bi-leader discharge and (2) the junction discharges composed of K-change processes. Fast recoil streamer discharges are also called K-changes and constitute the brightest cloud flash types. The physics are the same as for dart leaders, except that the K-changes propagate partially or completely within the channels initially ionized by both negative and positive leaders.

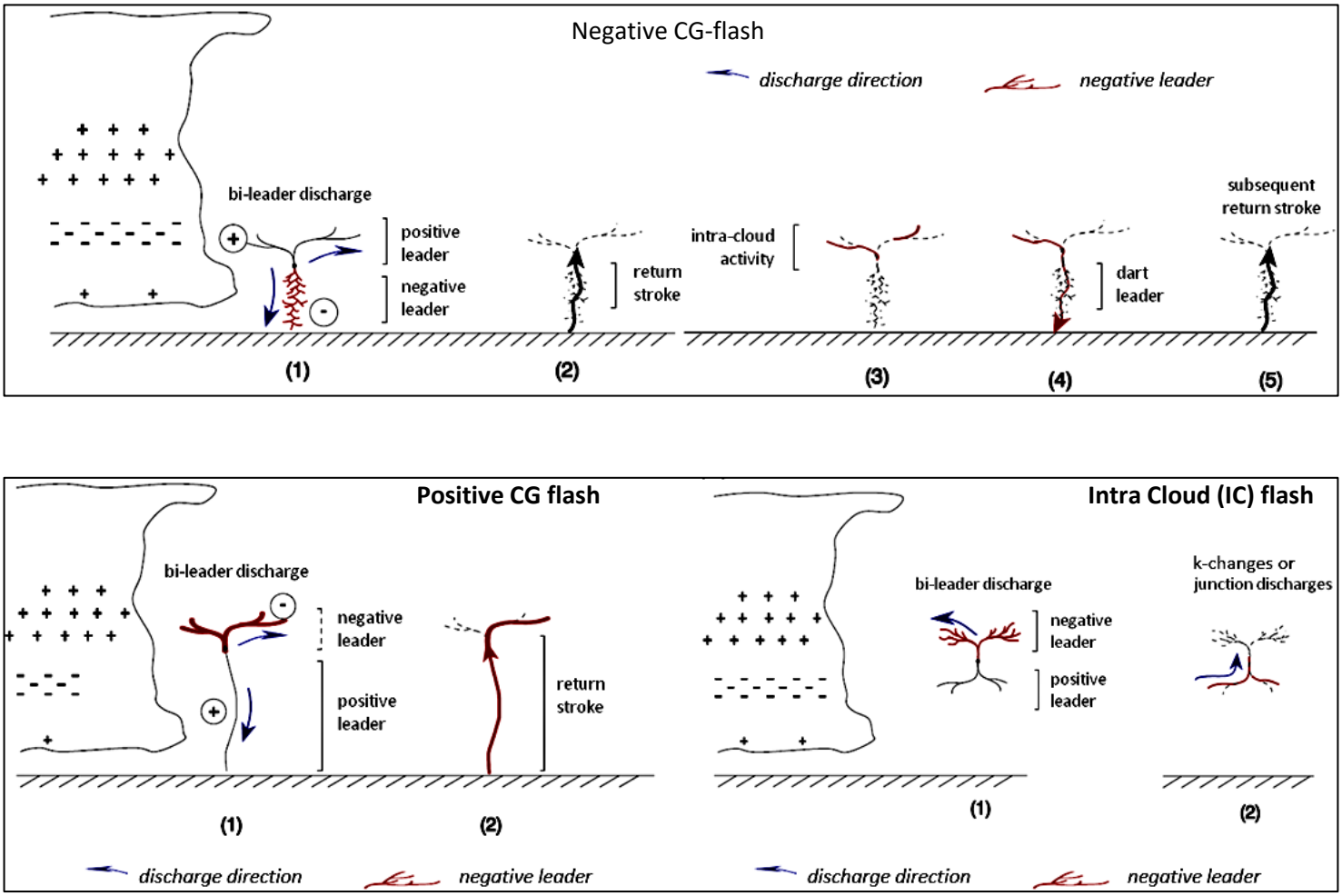

Fig. 1-5: Schematics of negative CG flashes (upper series), positive CG flashes (lower left), and IC flashes (lower right) adapted from Erdmann (2020).

As introduced above, flashes can be observed with different techniques. Every approach has its specific pros and cons. Optical sensors detect the emitted light pulses and suffer from clouds and hydrometeors attenuating the signal. Lightning Locating Systems (LLSs) operating on Low Frequency (LF) and Very Low Frequency (VLF) in national or global networks do best to detect vertical lightning channels and ground strokes. Very High Frequency (VHF) sensor networks (Lightning Mapping Arrays, LMAs) are only available for small regions but provide highly detailed three-dimensional data on discharges. LMAs are designed with ground-based antennas to detect lightning leaders in the VHF range by a time-of-arrival technique.

Acoustic and electrostatic field sensors are other ground-based systems sensitive to the thunder sound waves and local electrostatic field respectively. Due to a typically high acoustic noise and the small-scale nature of electrostatic field changes, those systems can only be applied locally. Table 1-1 below provides an overview of systems with at least regional coverage.

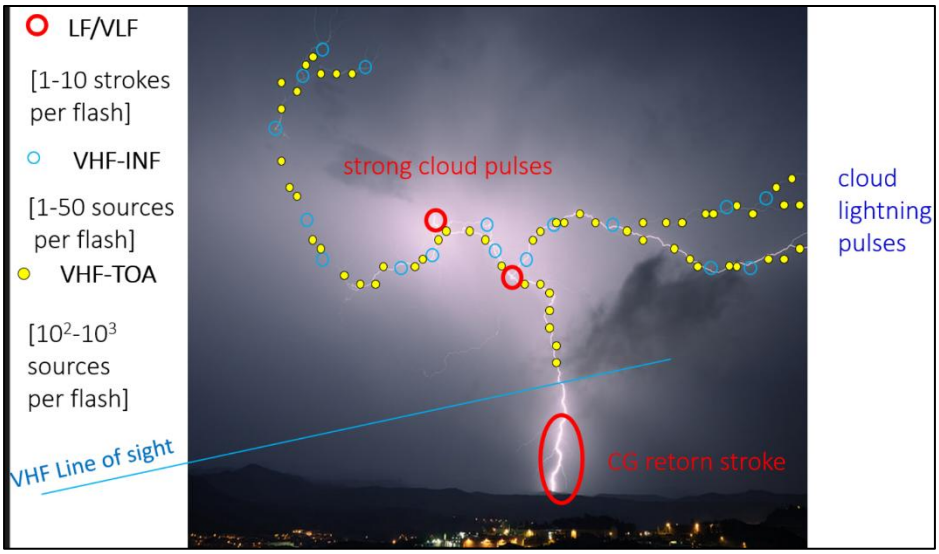

Fig. 1-6: Schematic illustration on typical detections by different radio frequency systems (Pineda, Montanayà, van der Velde, & López, 2023). Hundreds to thousands of sources can be detected for a single flash by a VHF-TOA system (LMA), dozens by a VHF-INF system, and 1 to 10 strokes per flash by a LF/VLF system. Detection of VHF signals requires a free line of sight.

Signal	Baseline	Detection capability	Attributes	Instrument/Network
VIS	**Space borne**	**80%-90% of CG+CC+IC**	**2D mapping and radiance GEO/LEO FOV**	• **Optical Transient Detector (OTD, 1995)** • **Lightning Imaging Sensor** • **(LIS, 1997)** • **Geostationary Lightning Mapper (GLM, 2016)** • **Lightning Imager (LI, 2022)**
VHF	10-20 km	100% of CG+CC+IC	Regional 3D mapping	• Ebro Lightning Mapping Array (ELMA) • Suivi de l'Activité Electrique Tridimensionnelle Totale de l'Atmosphère (SAETTA)
LF	50-300 km	50%-90% of IC+CC >95% CG	Europe coverage	• European Cooperation for Lightning Detection (EUCLID)
VLF	>1000 km	10%–30% CC+IC 70%–80% CG	Global coverage	• Vaisala GLD360 • Met Office Leela

Table 1-1: Characteristics of different lightning detection systems (courtesy of B. Viticchie)

Work by Montanayà, van der Velde, Pineda, & López (2019) shows that for flashes detected by LIS (a lightning imager instrument deployed at the International Space Station (ISS), source heights are quite variable, confirming that also flashes with sources at low altitudes can be detected by the lightning imager. Most flash sources were found at heights between 8 and 15 km though.

A comparison of LMA-based lighting flash detection and MTG LI data is provided in Figures 1-7, 1-8, and 1-9. One can see that both temporal and spatial consistency are excellent (Fig. 1-7). The detection ability of LI increases with altitude (Fig. 1-8). Fig 1-9 demonstrates a pleasing spatial collocation of LI and LMA detections. In the provided timeline, LI seems to be especially robust in detecting flashes with an extensive amount of LMA sources.

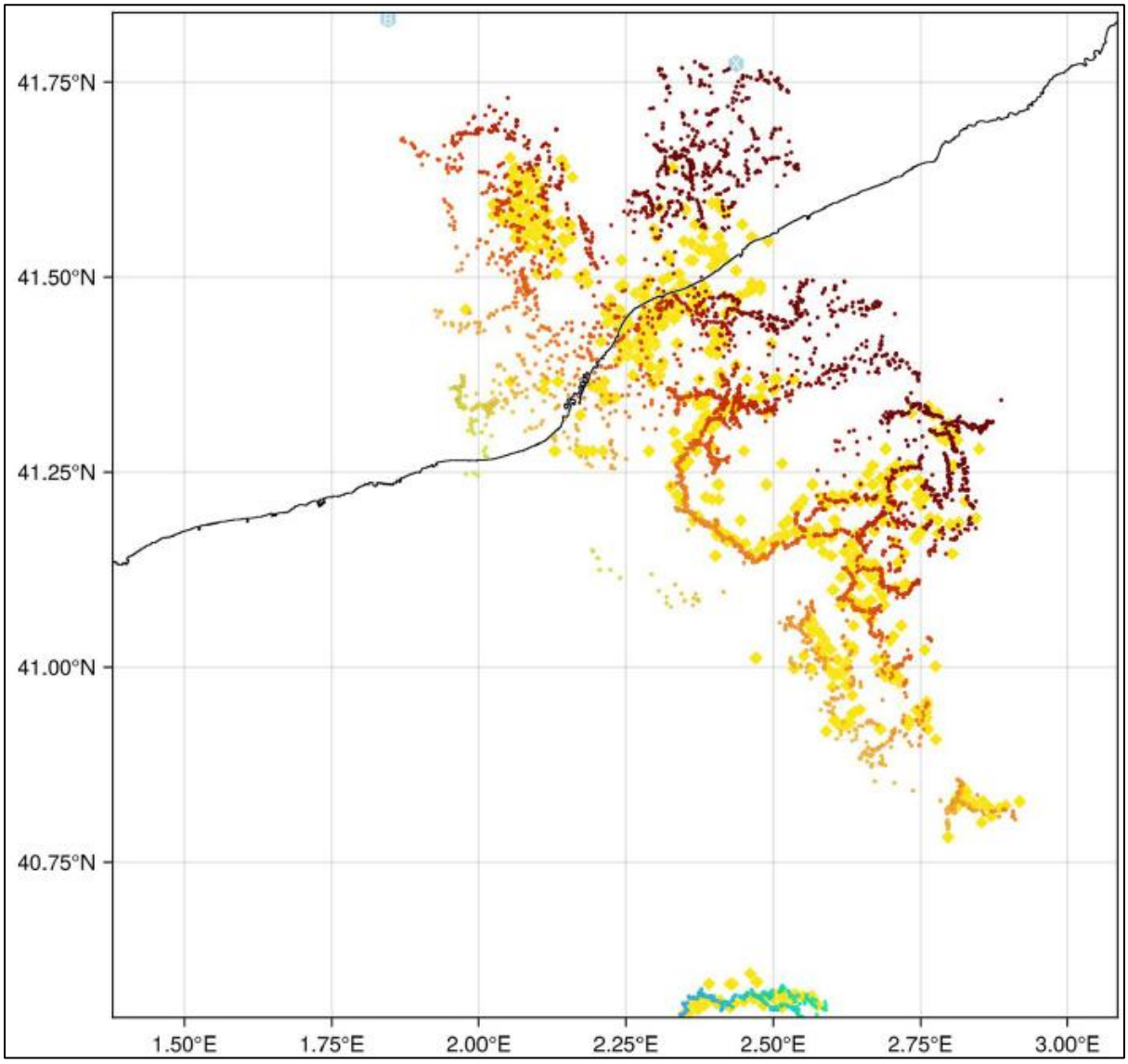

Fig. 1-7: Comparison between LMA data (small dots of darker, mainly reddish colour) and MTG LI data (large yellow diamonds) in the region of Catalunya, Spain, , on 14 August 2024, 01:53:42 to 01:53:46 UTC. Striking coherence of mainly the positive leaders was found between LMA sources and LI group detections (van der Velde, 2024).

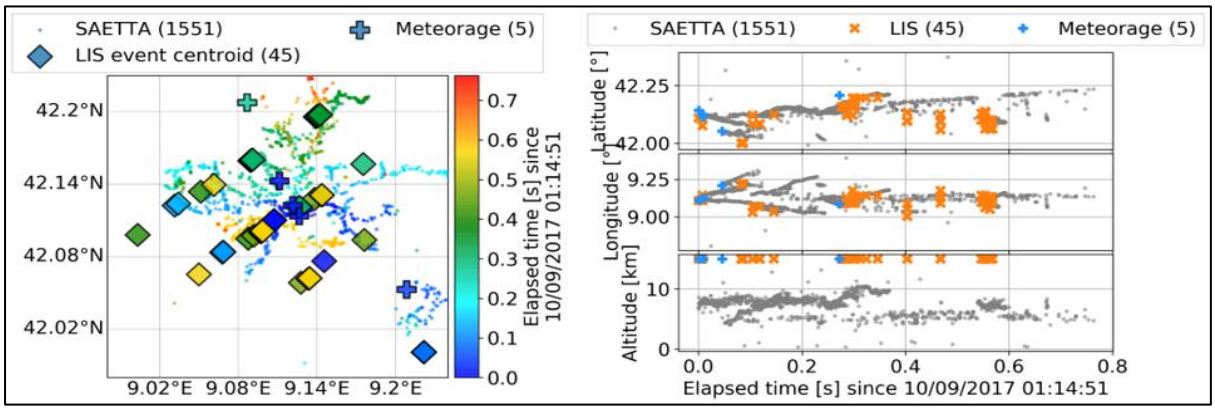

Fig. 1-8: LAT/LON-plot (left) and time versus LAT, LON, and altitude (right) with data from three different LLSs: SAETTA (an LMA installed on the island of Corsica), Meteorage (the national lightning data network in France), and LIS (the optical instrument on board of the ISS, as MTG LI proxy data). In this example, LIS captured significantly more lightning events than Meteorage, but not all phases of the discharges were detected. High reaching lightning channels are best captured by LIS events. (Erdmann & Poelman, 2023)

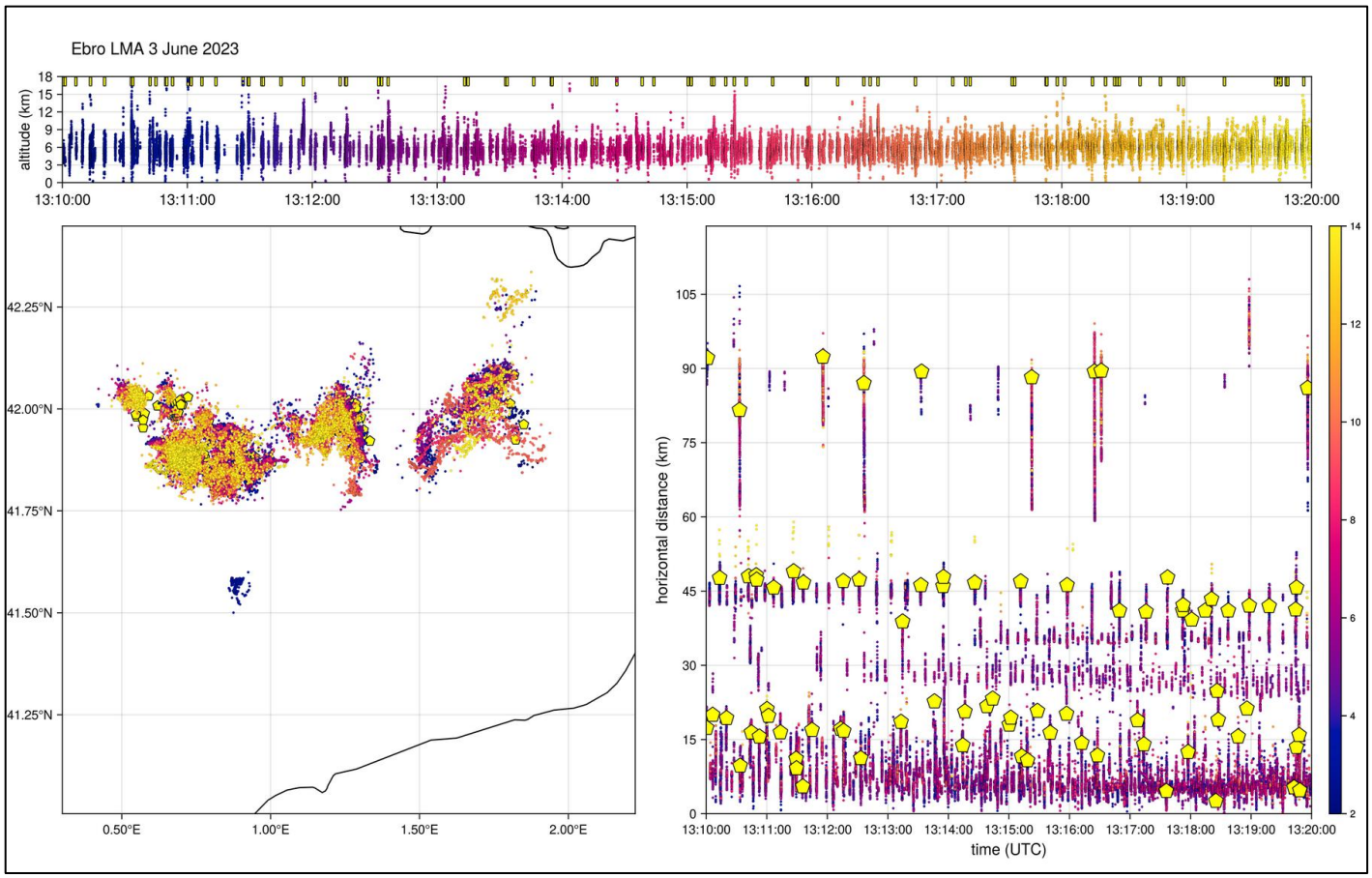

Fig. 1-9: 3 June 2023, 13:10-13:20 UTC. Top: time-altitude plot of LMA sources. Each vertical line is a flash. LI groups are shown as yellow bars. Left: map focused on central Catalonia. LI flashes are pentagon symbols, mostly covered by LMA sources, meaning they are well collocated. Right: time-distance plot with LI flashes as yellow pentagons. LI was operated in low-sensitivity test mode on that day. Unpublished work by van der Velde (2024).

LI detects transient optical pulses of milliseconds:

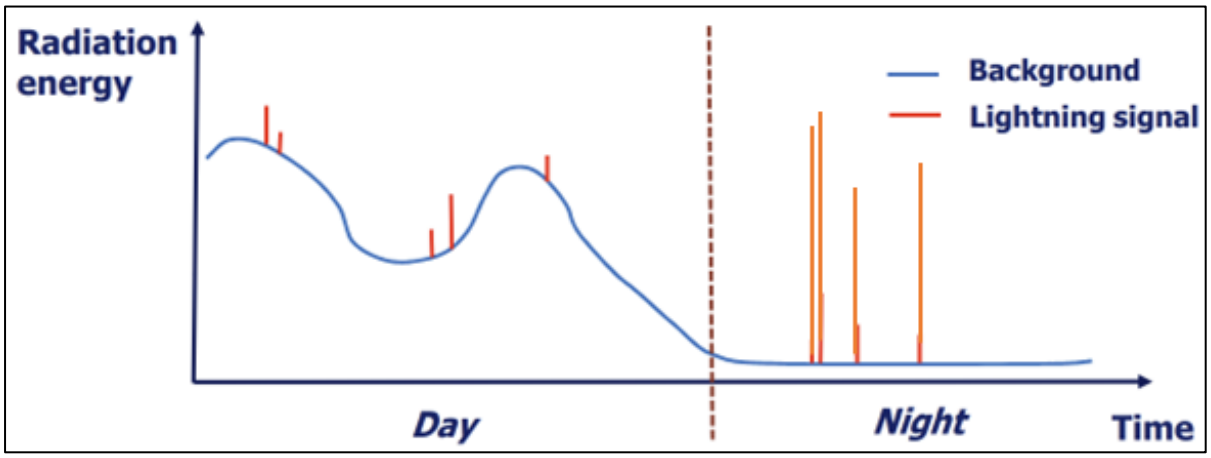

Fig. 1-10: Principle of the detection of lightning optical signals with a background signal changing with time. Lightning on top of a bright background is not recognised by its bright radiance, but by its transient short pulse character at a wavelength of ~777 nm. A variable adapting threshold must be used for each pixel taking into account the change in the background radiance. (Pohjola & Grandell, 2016)

The detection of lightning by LI mainly depends on its luminosity, governed by the amount of energy heating up the channel, and on the cloud optical properties above and surrounding the flash. Optically thick clouds can partly or completely attenuate the optical signal emanating from lightning. Orientation of a flash is also important, with increasing chances of detection for large horizontal components resulting in larger illuminated areas. Although CG lightning is typically more energetic than IC lightning, the strength of the detected LI signal might be dominated by the other factors. Effectively, a space-based optical sensor usually detects a combined lightning-cloud signal.

Understanding the fraction of the light reaching cloud top in a thunderstorm and where it occurs can help us understand how satellite lightning imagers are performing and how light propagates in a cloud (Brunner & Bitzer, 2020). It was modeled for two different scenarios, including a range of water droplets, ice particles, and their aggregates that change with height and location in the storm, that for a lightning discharge at 7 km altitude approximately 22 % and 13 % of light will reach cloud top in a thunderstorm. Light not reaching the cloud top is either absorbed or scattered toward another cloud boundary. The total amount of light that is not absorbed and escapes via one of the five alternate cloud faces (bottom, two X boundaries and two Y boundaries) due to a 7 km source is case-dependent between 50 to 85 %.

Rimboud et al. (2022) succeeded in simulating lightning images and thereby support our understanding of light occultations, light emittance via surrounding clouds and surfaces, or directly from the upper part of the clouds:

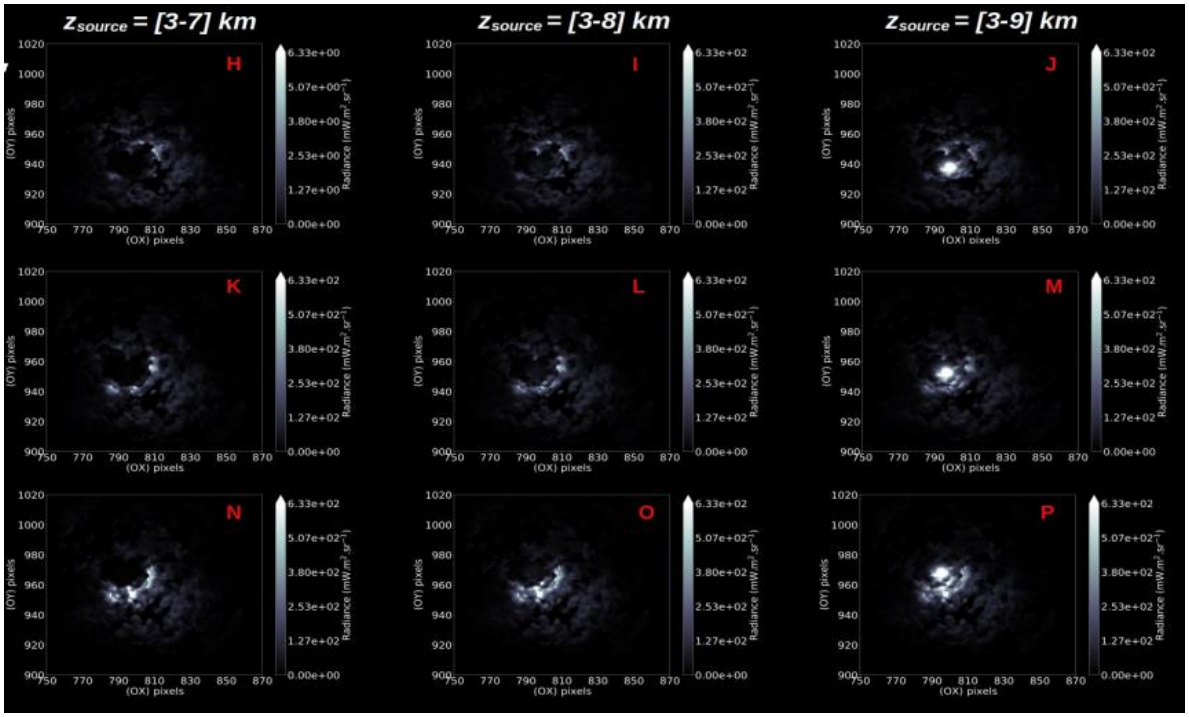

Fig. 1-11: Simulations of visible light emittance (view from top) depending on the viewing angle (upper row from northern angle, middle row from zenith, lower rom from southern angle) and height of the lightning discharge within the cloud column (from lowest in left column to highest on right column). (Defer, et al., 2023) and (Rimboud, et al., 2022)

It is generally easier for the optical signal from flashes to emerge from isolated and small cells than from large convective complexes. Detection of mainly vertically oriented flashes becomes more probable if such flashes happen at the edge of storms and are seen from the side. Especially with severe thunderstorms, flashes can be detected by both cloud-top and side-wall detections (see examples in Fig. 1-13 and Fig. 1-14), leading to spatially separated maxima of LI detections: one near the overshooting top, another one near the anvil edge.

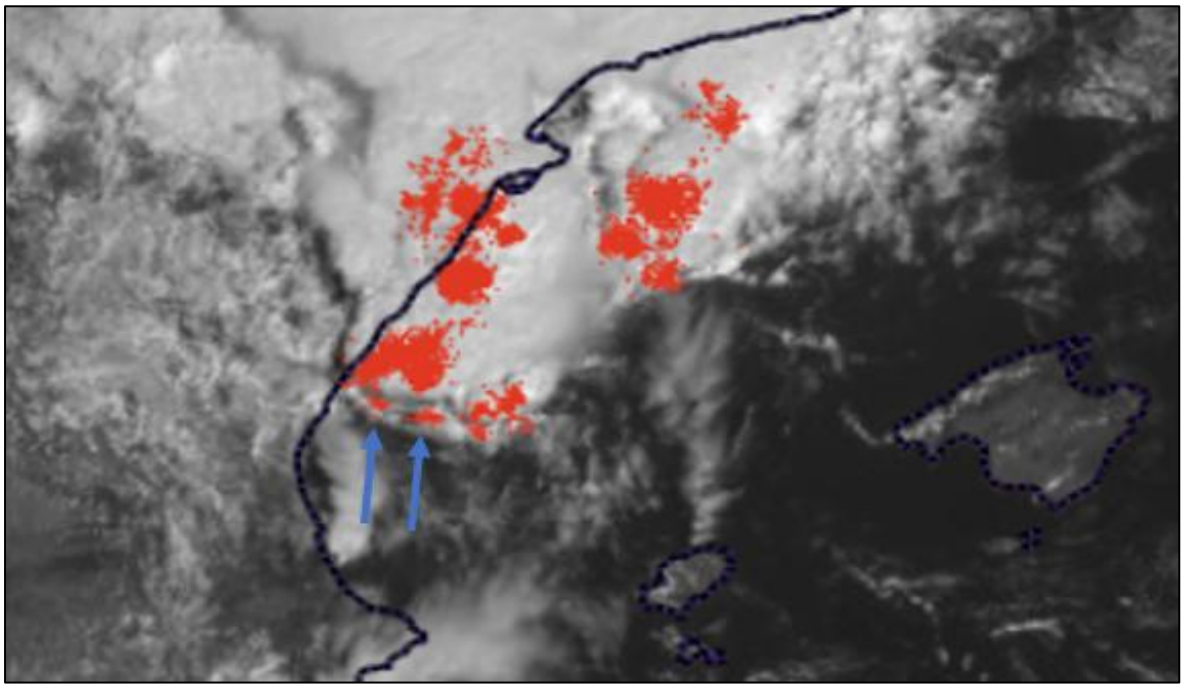

Fig. 1-12: Thunderstorms near the coast of Catalonia, Spain, on 3 September 2024 at 10:00 UTC. Blue arrows marking LI detections (LI Groups indicated by red dots) that probably originate from the southern sidewalls of the clouds and/or anvil edge. The related active updrafts with the majority of cloud-top detections are located several kilometres further north. Background: FCI high-resolution 0.6 micron visible channel. Screenshot from ESSL Weather Displayer.

More difficult to detect are cases where deep clouds attenuate the flash signal. For (isolated) storms near the edge of the field of view, LI might see a full side view of the storm and sometimes even the exposed lightning channel between the cloud and the ground (very bright). This is impossible if there is widespread cloud cover of course.

Fig. 1-13: Video still from MUNINN MISSION ISS BROLL Thor-DAVIS Thunderstorm Observation from space. Example for visual appearance of flashes with light being both emitted from top and lower side- parts of thunderclouds. (ESA – M. Wandt, 02/2024)

Chapter 2: The Meteosat Third Generation Lightning Imager (MTG LI) and its data properties

The MTG LI was launched in December 2022 and is on board of the MTG-I1 satellite and provides continuous optical observations of lightning:

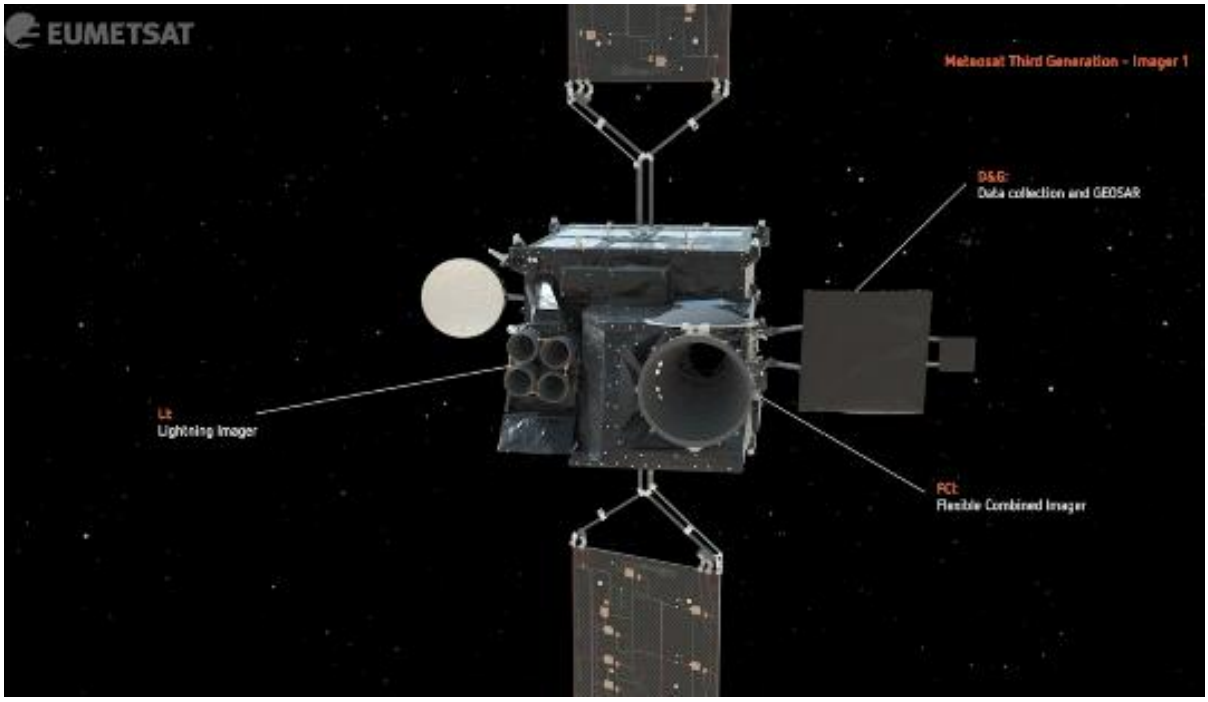

Fig. 2-1: Visualization of MTG-I1 in orbit. (Bojinski, 2023)

LI in a nutshell	
Spatial Resolution at Nadir	**4.5 km (variable throughout the Field of View, FOV)** compare: 8 km for GOES-GLM
Spectral band	**777.4 nm and 1.9 nm narrow band**
Detector(s)	**1000 x 1170 pixel (x 4) CMOS**
Frame rate	**1 ms (1 kHz acquisition frequency –** double than for GOES-GLM**)**
On-board processing	• **Background evaluation and subtraction** • **Lightning detection** • **On-board filtering**
Bandwidth	**30 Mbps**

Table 2-1: Basic setup of the lightning imager (Bojinski, 2023).

Field of View (FOV) projection:

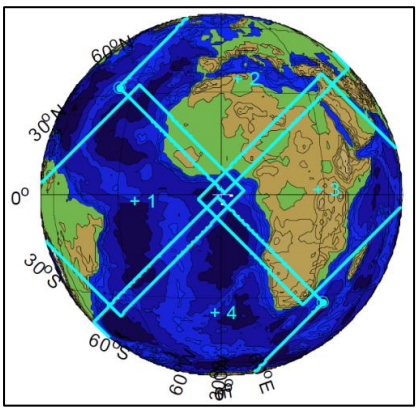

Fig. 2-2: Four cameras are directed towards the earth and cover most of the disc that is visible from the MTG orbit. All of Europe lies within the northern camera, i.e. within a single detector coverage. At 60 ° latitude the spatial resolution will be around 10 km. Schematic for 0 ° longitude satellite position.

LI data content (basic data not disseminated as level 2 data)

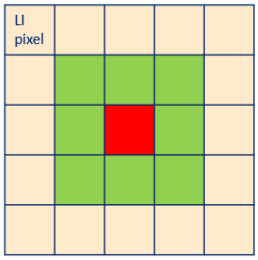

LI Event (or Detected Transient) with 3x3 window

Pixel-sized energy measurement above the detection threshold (at RTPP)

This is the basic component of the optical pulse detection of LI and is the basic component of the data processing from Level 0 to Level 2

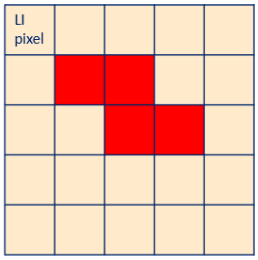

LI Group

Collection of connected DTs on a single acquisition frame

This is an optical pulse detected by LI in one frame. Groups are defined and analyzed at Level 2

Fig. 2-3: Schematic for LI Event and LI Group composition.

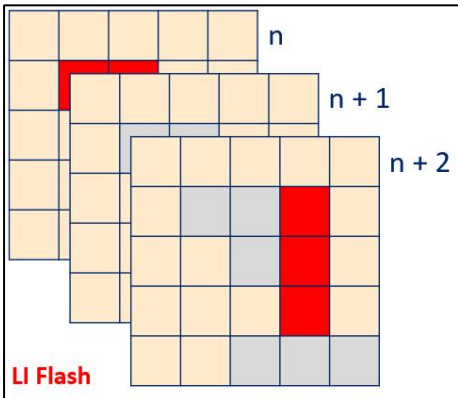

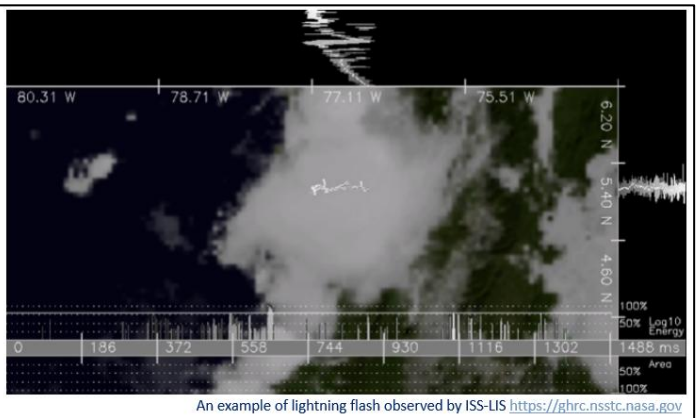

An example of lightning flash observed by ISS-LIS https://ghrc.nsstc.nasa.gov

Collection of groups that are correlated in space and time

This is a collection of optical pulses (detected as groups) correlated in space and time. Flashes are defined and analyzed at Level 2

Fig. 2-4: Schematic for LI Flash composition. The ISS-LIS example on the bottom right denotes an extreme case with a long duration flash that extended over a large distance. Typically, LI mapped flashes will rather consist of a few pixels only.

The following 5 products are disseminated as level 2 data with a nominal timeliness of 90 s.

1) Point data

The **LI-2-LGR**-BODY **Group** product provides **groups as points** that should be considered as **counterpart of the ground-detected strokes** and are provided every 10 s in NetCDF format (data provided at the native resolution of 1ms, chunked in files covering 10 s each). The point is a geographically weighted average (centroid) of pixel events.

The **LI-2-LFL**-BODY **Flash** product provides **flashes as points** that should be considered as **counterpart of the ground-detected flashes** and are provided every 10 s in NetCDF format (data provided at the native resolution of 1ms, chunked in files covering 10 s each). Flashes are a collection of groups correlated in space and time (over 330 ms).

The flash position is the radiance-weighted centroid of the positions of the events being within the groups of the flash (see Fig. 2-4 bottom).

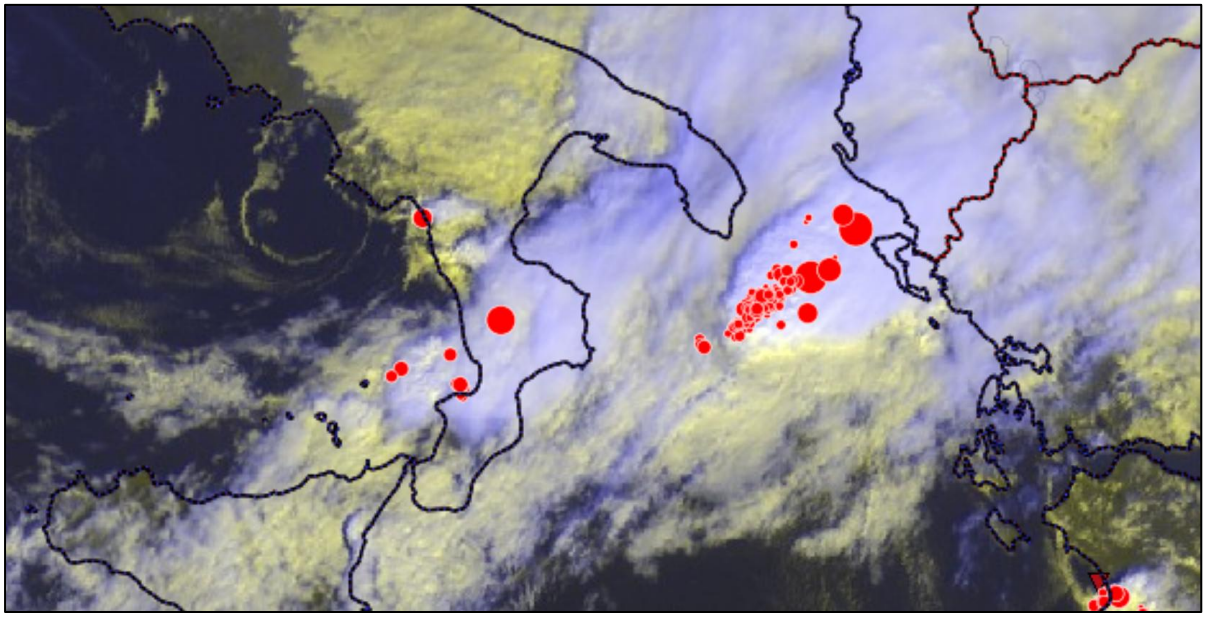

Fig. 2-5: Example for point data visualisation. Convective activity over the southern Mediterranean Sea at 09:25 UTC on 13 July 2023. Red dots of different size: LI flash area point data, 5-minute bin, plotted on top of HRV-Clouds product from SEVIRI. The red dot radius is proportional to the logarithm of the flash area, which the LI data includes as a flash property. Significant fraction of large flashes over the area between southern Italy and Greece. Image source: EUMETSAT, ESSL Weather Data Displayer, from (Holzer, 2024).

2) Gridded accumulated data

The **LI-L2-AF** Accumulated **Flash** product allows to keep track of the **density of events within sequences**. The product provides accumulated events normalized by the total number of events in the flash itself (computed for all the flashes). It thereby **highlights regions of more frequent flickering within each flash**. Provided every 30 s.

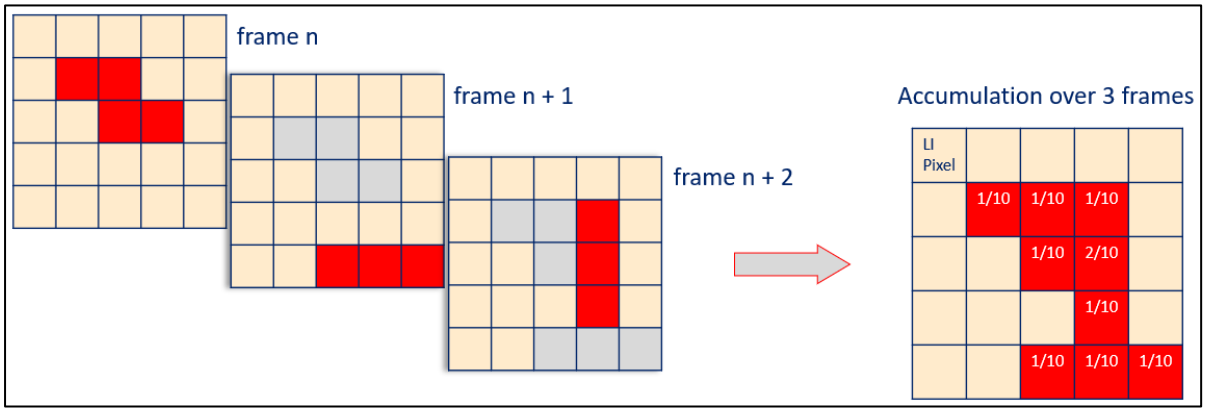

Fig. 2-6: Schematic of LI-L2-AF Accumulated Flash product composition.

The **LI-L2-AFA Accumulated Flash Area** product allows to keep track of the **areas touched by flashes**. It provides information on the **extent and frequency of flashes per pixel** but not on the frequency of events (or detected transients) per pixel (which would result in much higher quantities). Provided every 30 s.

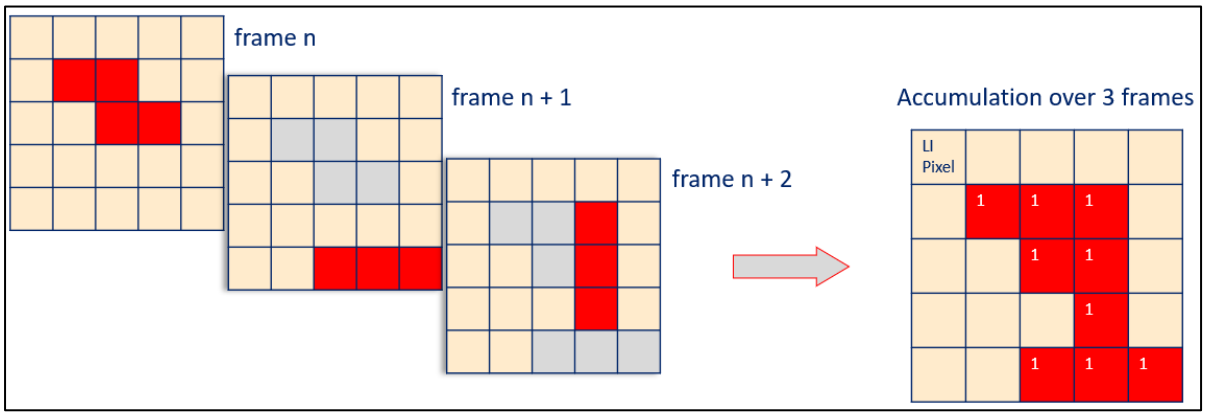

Fig. 2-7: Schematic of LI-L2-AFA Accumulated Flash Area product composition.

The **LI-L2-AFR Accumulated Flash Radiance** product represents the **total radiance** detected **within a certain pixel from multiple events**. Provided every 30 s.

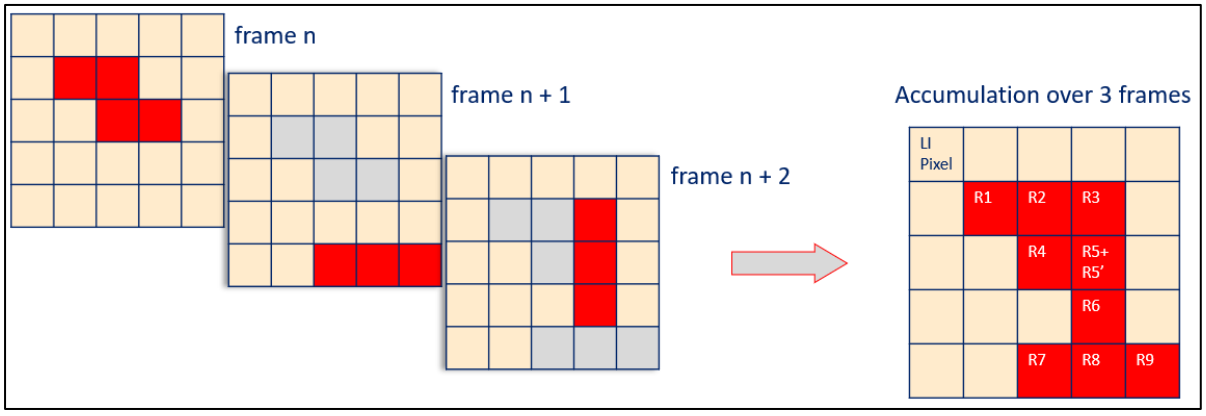

Fig. 2-8: Schematic of LI-L2-AFR Accumulated Flash Radiance product composition.

Sub-pixel or pseudo-high resolution of LI point data

LI Group and LI Flash point data inherits a downscaling effect (sub pixel grid resolution or pseudo-high resolution) that is based on physical properties. Centroids are calculated on the basis of radiance weighting of pixel values, i.e. the LI events. The radiance weighted centroids pick up brighter parts of the cloud lit up by lightning, and thereby constitute not only a random procedural data manipulation.

This effect helps recognize features in severe storms that we know from LMA data too, for example lightning holes in the overshooting top region. If only data on the pixel grid would be available, such effects could hardly be seen as their scale is typically smaller than the raw data grid resolution.

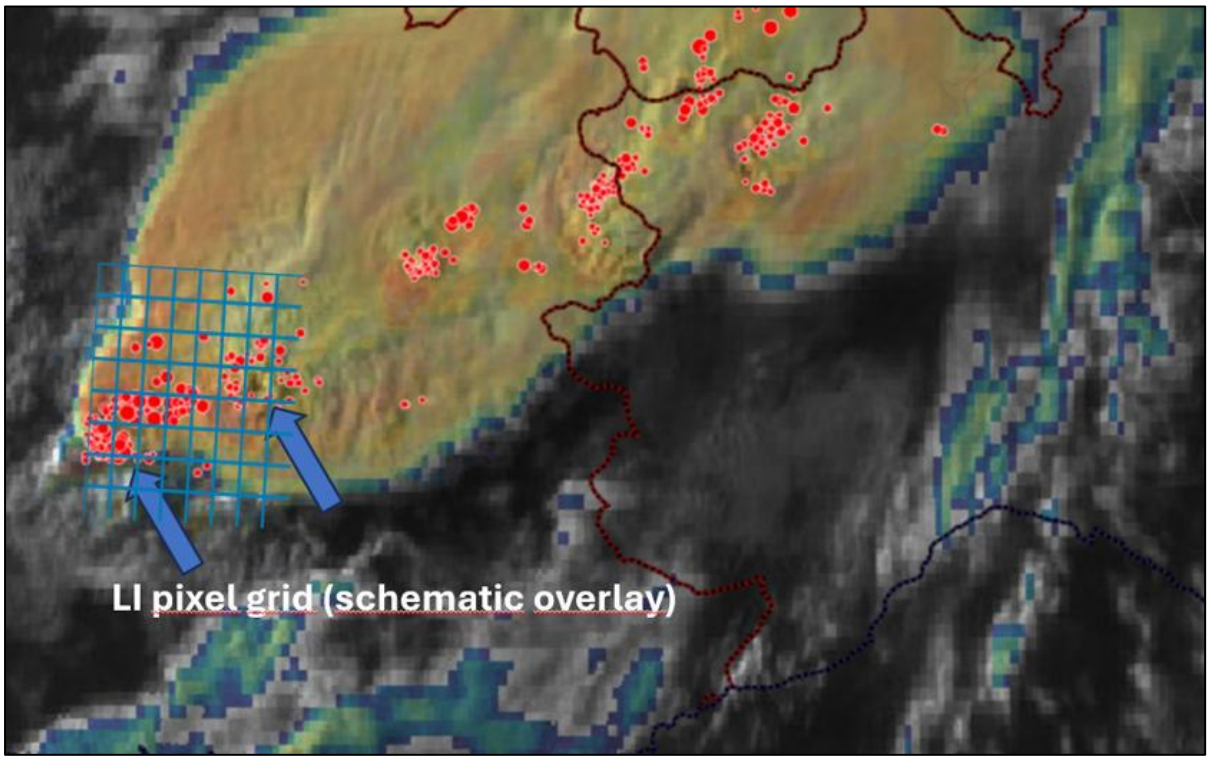

Fig. 2-9: Radiance weighted LI point data centroids can deliver relevant information for forecasters on a much finer scale than the original pixel grid. Example of 12 July 2023 at 18:00 UTC for flash sizes over southeastern France. LI Flashes (size of circles relates to flash size) on SEVIRI Sandwich background.

Detection Efficiency (DE)

Due to the limited period of validation by the end of 2024, information on the LI detection efficiency (DE) still needs to be seen as preliminary.

Since there is no absolute reference[2] for lightning occurrence in the atmosphere, DE is determined relative to a reference dataset (typically data from the surface-based lightning detection system GLD360) which has a limited DE too. This means that LI can detect flashes that are not detected in the reference dataset. In addition, due to the nature of LI data, correction of parallax effects is a challenge for the proper attribution of LI events to reference data and can result in a threshold-dependent degradation of DE metrics. This effect is most prominently seen in high latitudes or towards the edges of the LI field of view (FOV), although LI does see a lot of lightning even in such areas.

From first principles and GLM experience, we know that the DE depends on the time of day. Additional important factors are the size and duration of flashes, the optical thickness of clouds and hydrometeors in the line of sight between the light-emitting event and the optical instrument (see section "MTG LI Measurement Principles" in chapter 1 above), and availability and albedo of reflecting clouds or surfaces.

Zhang & Cummins (2020) found for GOES-GLM relative to high-quality data from the Kennedy Space Center Lightning Mapping Array (LMA) in central Florida - while an LMA is significantly surpassing the DE of typical national Lightning Detection Systems, that the mean daily flash DE was 73.8 %. GLM reported 86.5% of the LMA flashes that had coincident cloud-to-ground return strokes reported by the U.S. National Lightning Detection Network. Results also reveal that flash size and duration are critical parameters influencing GLM detection, regardless of the storm type, with 20–40% detection for small and short-duration flashes and greater than 95% detection for very large and long-duration flashes. For LI, no such validation data for longer periods is available yet.

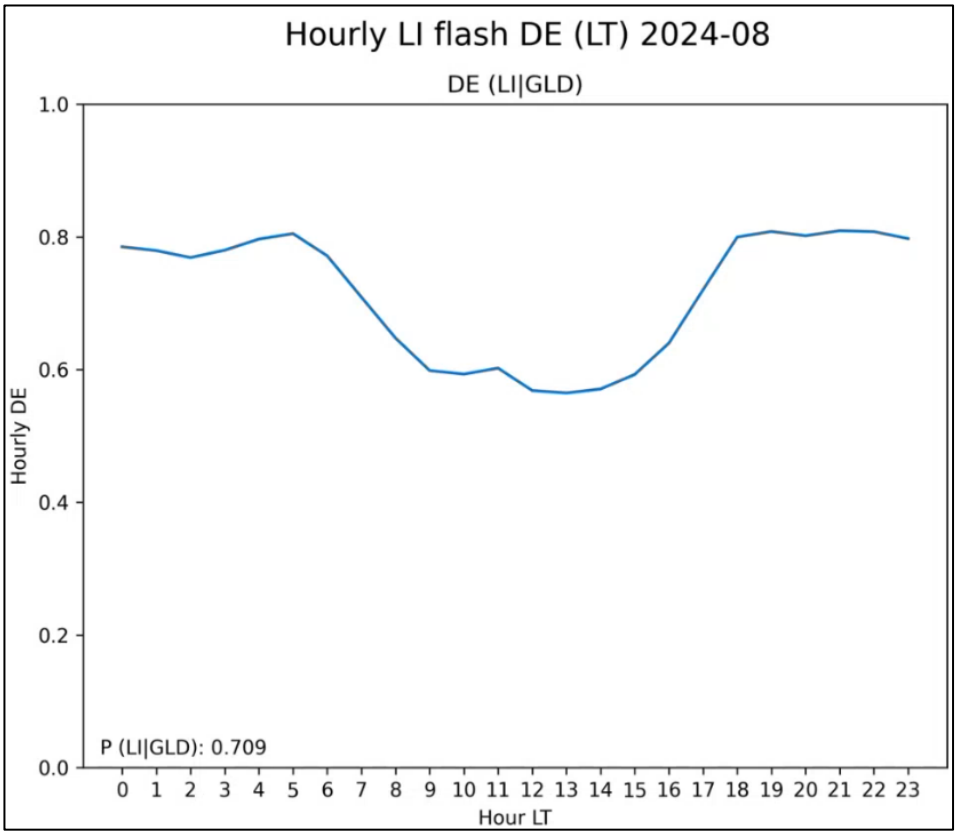

Fig. 2-10: Daylight dependency of LI Flash DE for August 2024. Preliminary results based on short observation periods. Source: EUMETSAT.

[2] Lightning Mapping Arrays (LMA) are the closest to an absolute reference, available only in a few locations.

The LI location accuracy is currently measured by using LI groups and comparing them to GLD360 strokes. For each matching pair, the 3 components are measured. The absolute (straight-line) location offset, the North-South component and West-East component offset. The average SEVIRI ice cloud top height is used for the parallax correction. It is unknown how the location accuracy is distributed over the FOV for the ground-based systems. For the limited amount of data available, the small spatial offset for event-groups compared to GLD360 is well noted. Over large parts of Europe and Africa, mean North-South location offsets compared to GLD360 are below 5 km, mean west-east offsets around 5 km (see Fig. 2-11).

For a 16/17 October 2023 case, a median location offset of only about 3.5 km was found for W-E and N-S location at Level 1b for southern Europe.

Probably less than 0.1 false LI Flashes per second are detected in the FOV, mainly over the tropical Atlantic Ocean. In general, false detections are very rare.

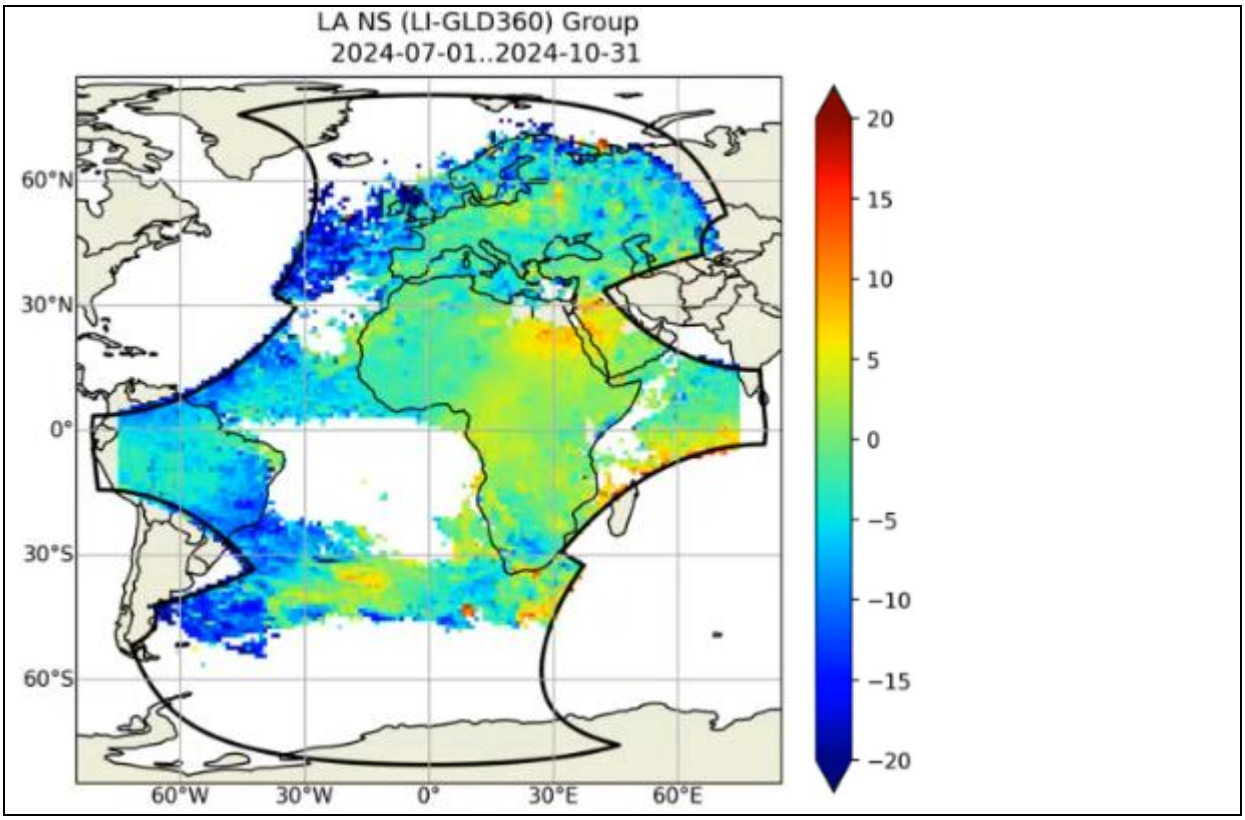

Fig. 2-11: LI Group North-South mean location accuracy (km) for July to October 2024 relative to GLD360 locations. Source: EUMETSAT.

Relative to EUCLID data, the median location delta for LI events from a 2023 test data sample is 3.3 km. This value is smaller than the native resolution of the LI pixels over the EUCLID domain, i.e. the LI/EUCLID comparison confirms the GLD360 validation results.

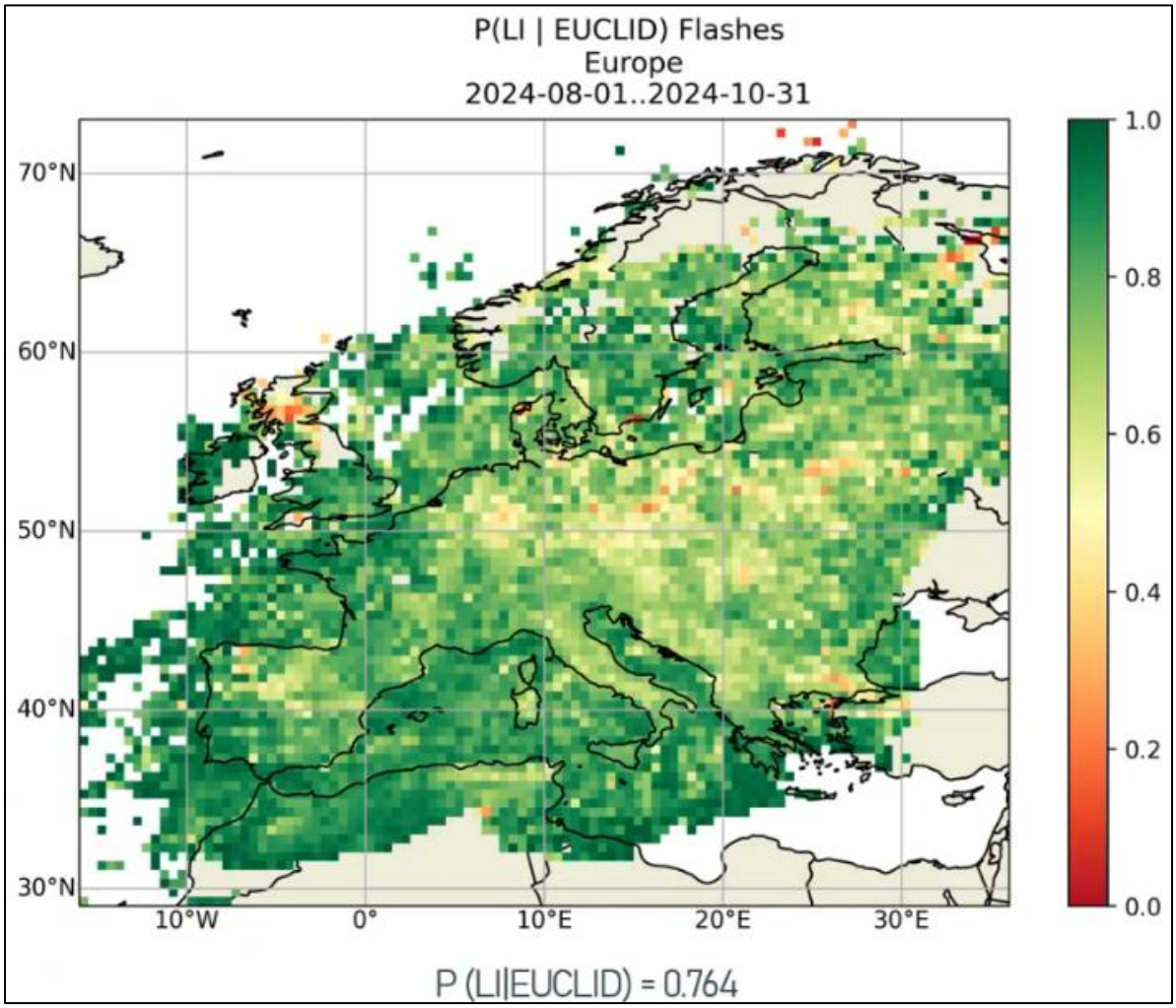

Fig. 2-12: LI Flashes DE relative to EUCLID Flashes. Data for July to October 2024. Local minima are often related to small sampling sizes. Source: EUMETSAT.

For the latest LI performance metrics, we kindly refer the reader to the latest version of the LI L2 Product Validation Report on the EUMETSAT User Portal:

https://user.eumetsat.int/s3/eup-strapi-media/LI_Level_2_Data_Operational_Dissemination_Validation_Report_pub2_bd35cd8ccf.pdf

Chapter 3: Visualizing LI data

Point products were found to provide complementary information to the ground-based lightning detection systems and valuable information for the forecasters in the nowcasting operations.

LI Flash or LI Group size and density can be used for early identification of relevant processes that lead to intensification of thunderstorms and ultimately to severe weather events. While the identification of an elevated potential for heavy rain, convective wind events and tornadoes needs to be further examined, the potential for large hail warnings is already obvious based on early data analysis.

LI Group and Flash point data inherits a downscaling effect (sub pixel grid resolution or pseudo-high resolution) that is based on physical properties (centroids on the basis of radiance weighting of pixel values / LI events) and not a pure procedural data manipulation effect. I.e. the radiance weighted centroids pick up brighter parts of the lit-up cloud. This effect helps to recognize features in severe storms that we know from LMA data too, for example flash holes in the overshooting top region.

Due to the high optical thickness of clouds in the active updraft regions, anvil edges can become preferred zones for light emittance. This effect is mostly found with exceptionally intense thunderstorms, i.e. could offer potential for severity pattern recognition by forecasters.

In addition to the nowcasting use, point products can also be used to produce overview maps of large geographical areas and/or timeframes of several hours or longer. Graphics and loops for media can be produced too.

Exemplary point data products

1) Group

(LI-2-LGR-BODY Group product)

The product delivers points that should be considered as **counterpart of the ground-detected strokes** are a centroid of instantaneous connected pixel events.

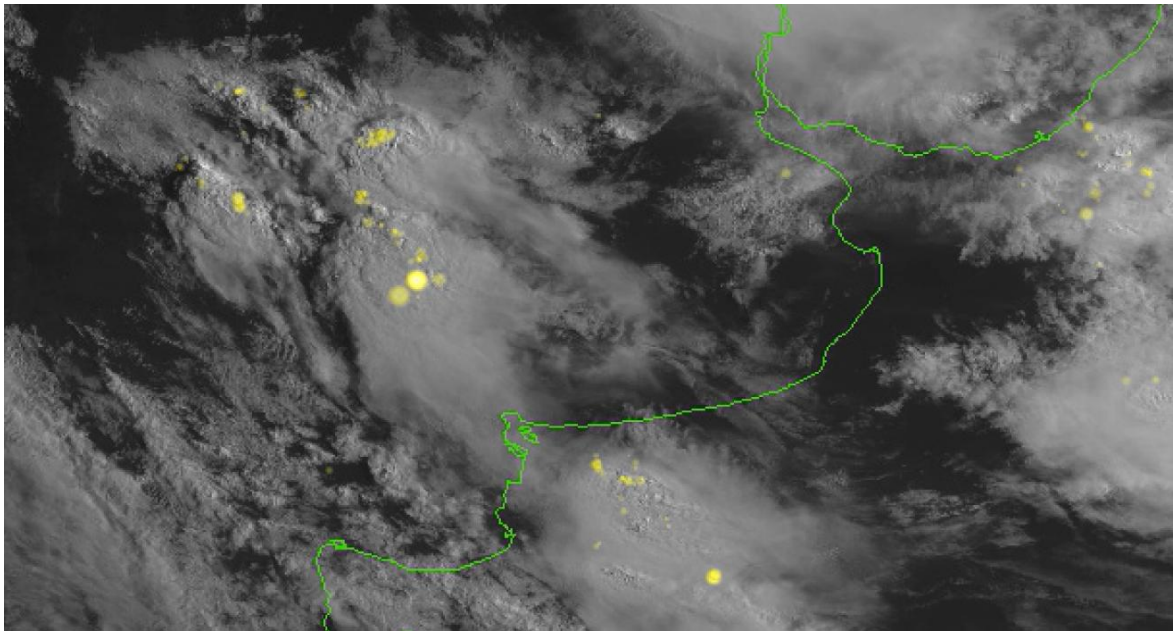

Fig. 3-1: Groups or flashes (both possible in this Meteo-France application) as single-colour balls (colour can be chosen) for media applications (TV channels). The ball size is an indicator of the covered area. The opacity is an indicator of the optical energy (high energy goes with high opacity). Visualization by Meteo-France. (Le Moal, 2023)

2) Flash

(LI-2-LFL-BODY Flash product)

The product delivers points that should be considered as **counterpart of the ground-detected flashes** and consists of a collection of sometimes 100s of groups correlated in space (16.5 km) and time (330 ms).

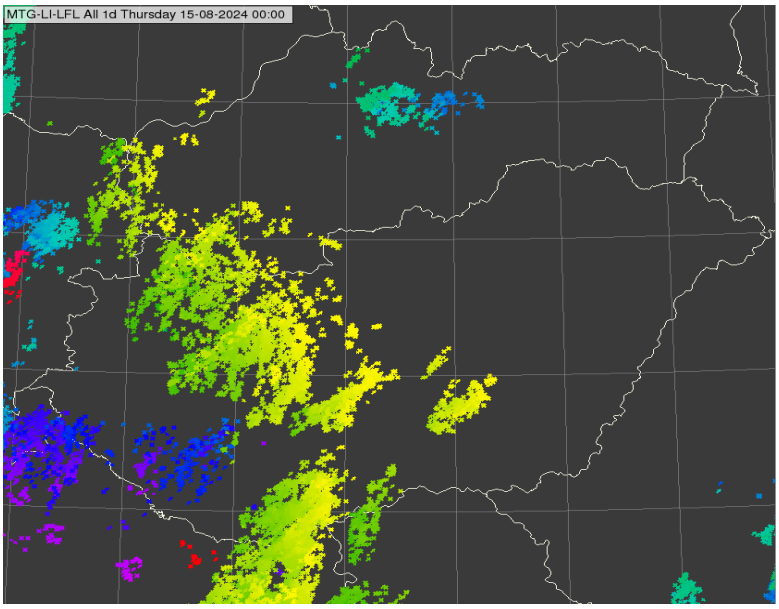

Fig. 3-2: Flashes as points colour-coded by time provided as a full-day overview (14 August 2024, 0 to 24 UTC). Map area: Hungary and surroundings. Courtesy of Zsofia Kocsis, HungaroMet.

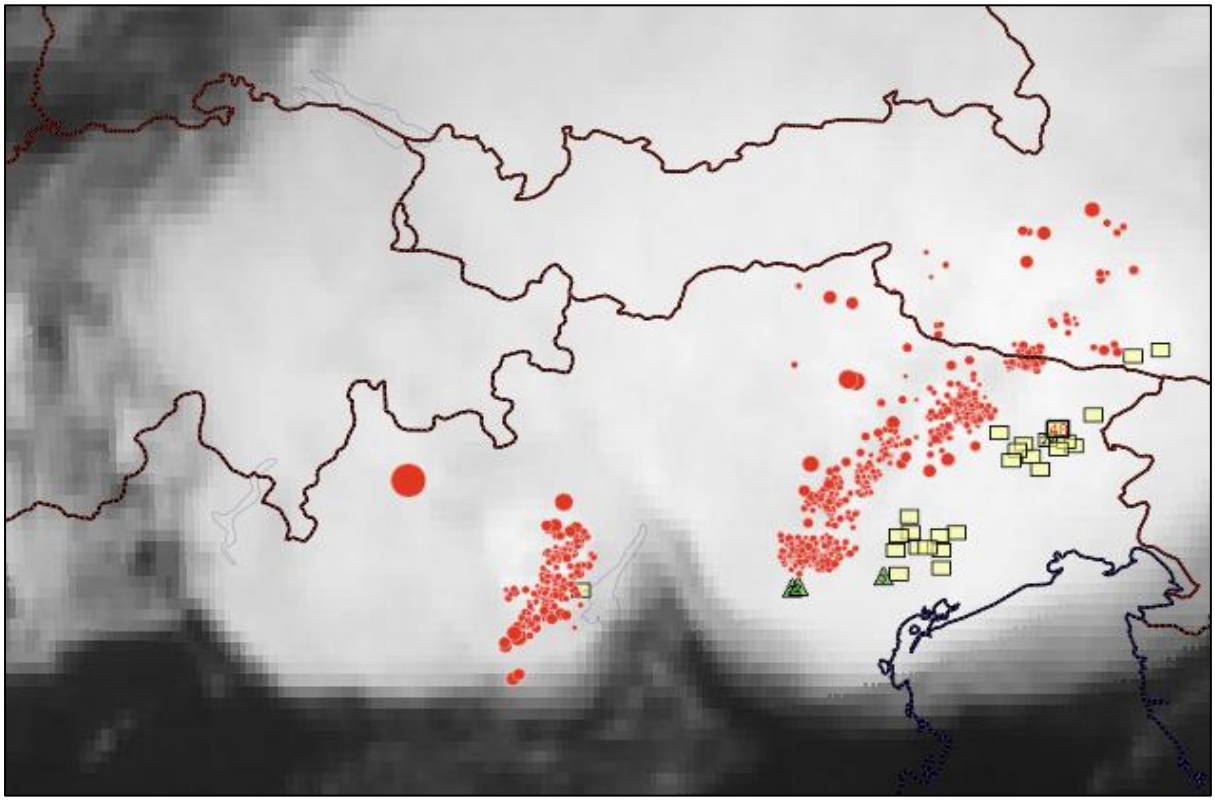

Fig. 3-3: Example of point data visualisation for 23:15 UTC on 12 July 2023 over northeastern Italy and neighbours. LI flash area plotted on top of SEVIRI IR 10.8. ESWD damaging wind gusts (yellow squares) and large hail events (green triangles) for the following hour. Red dots of different size: LI flash area point data, 5-minute bin. The red dot radius is proportional to the logarithm of the flash area, which is given as a property of a flash. Small flashes can be primarily seen with hail-producing cells and fresh developments, large flashes in the stratiform areas of the convective systems. Image source: EUMETSAT, ESSL Weather Data Displayer, from (Holzer, 2024).

Gridded data products

The EUMETSAT accumulated baseline products (AF, AFA, AFR) are based on the event level. In the very short time available for analysis in the year 2024, additional value that originates from the event level compared to the group level (available through the point products) was not found for the purposes of nowcasting so far.

The experimental ESSL group level gridded product visualizations ("Group density gridded" and "Geometry and density") were found useful in looking at the cases by experts and forecasters during the testbeds and expert workshops.

Single examples showed that AFA, AF, and AFR maxima can, out of a regional sample, highlight different thunderstorms and not necessarily the most impactful ones in a consistent way. More study is needed to confirm the forecaster usability of AFA, AF and AFR.

Workshop participants believe that there is potential for accentuating the most active and thereby most warning-relevant updrafts of convective systems by a product that highlights areas with frequent but small flashes. Such a product isn't available yet but will be developed and tested over the year 2025.

Background: Why we are interested in a high number of small flashes

The experience acquired from the LMA data shows that intense convective updrafts, often found in supercells, create large amounts of small charge pockets on the outskirts of the updrafts. As the charge is replenished in these charge pockets very fast, the lightning activity of such storms can consist of very frequent flashes that are small in size and energy. The LMA data show that the lightning activity in supercells can reach hundreds of flashes per minute, resulting in quasi-continuous light-emitting events (or sources from the LMA perspective). Therefore, collocation of a high density of flashes and a high fraction of small flashes can be a valuable indicator of strong updrafts capable of severe weather and possess high value for nowcasting warning operations.

In the ideal case, LI can detect a high quantity of light pulses in such cases while the lit-up areas are small. A number of factors could prevent LI from detecting the effect properly:

- The quasi-continuous light emittance could fool the base state detection algorithm, i.e. the assumption of a bright surface would be taken as background state, while in reality it is a quasi-continuous light emittance from small flashes, i.e. not so transient transients to be detected.
- The light emittance is too weak to surpass the sensor threshold, i.e. not enough photons are being emitted and received by the sensor cavity array.
- The optical thickness of the clouds between the light emitting event and the cloud boundary is high and light scattering and diffusion result in a too strong reduction of emittance on the top or side of the cloud to be detected by LI.

While single small flashes can happen with different storms, only a situation with both high density and high fraction of small flashes is of relevance for the nowcasting and warning purposes.

Thus, a gridded product to highlight such a coincidence and thereby the most dangerous convective updrafts, needs to include information on the frequency of small flashes. Possible ways to do this are showing the count of flashes below a certain flash size threshold or developing a Minimum Flash Area product considering areas with substantial flash activity only, i.e. by blending out results for areas with few flashes. Which of these or other variants is the most useful requires further study, focusing on the statistical properties of the currently detected flashes.

1) Accumulated Flash

The LI-L2-AF product shows the density of events within sequences. It provides accumulated events normalized by the total number of events in the flash itself (computed for all the flashes). **Highlights regions of more frequent flickering within each flash.**

2) Accumulated Flash Area

The LI-L2-AFA product delivers pixels/**areas touched by flashes**. It provides information on the **accumulated footprint of all the flashes**.

3) Accumulated Flash Radiance

The LI-L2-AFR product represents the **total radiance** (optical energy) detected and **accumulated within a certain pixel from multiple events**.

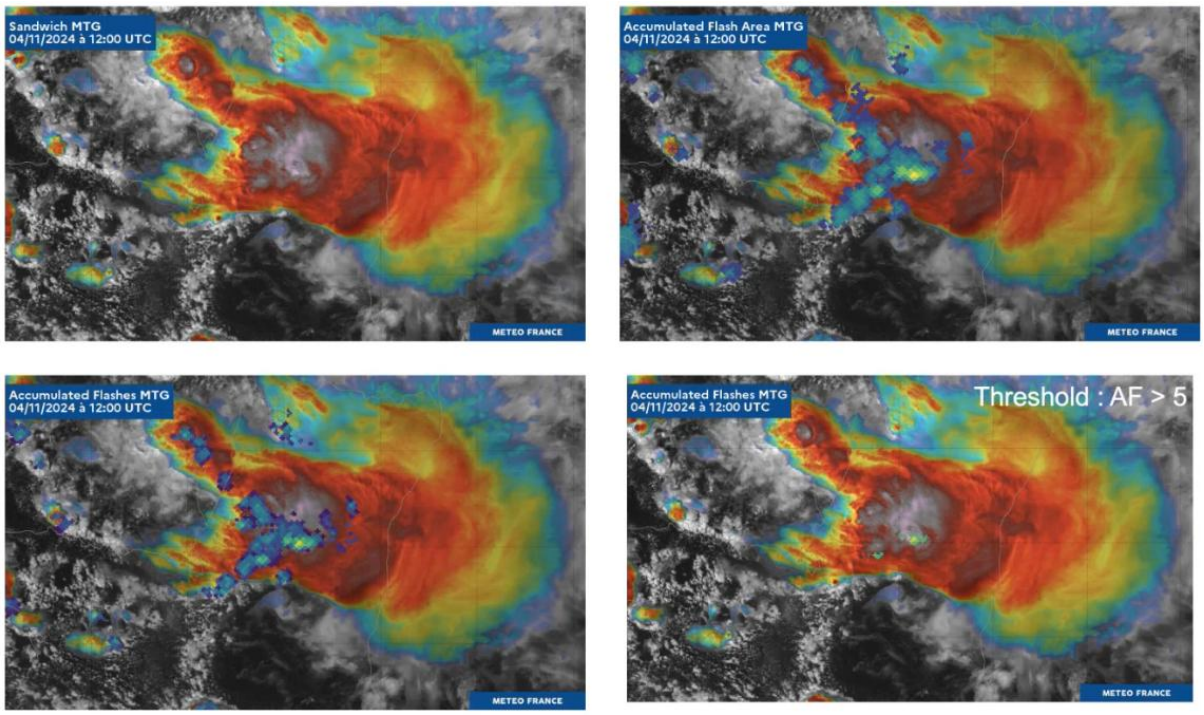

Fig. 3-4: MeteoFrance visualization of MTG FCI Sandwich (upper left), overlay of AFA (upper right), AF (lower left), and AF larger 5 (lower right). Source: MeteoFrance.

The interpretation of the Accumulated Flash Radiance (AFR) product is complex, and signals are misleading if taken as direct indication for the most active cells. In fact, optical energy (brightness of a pixel) is not correlated to the most active parts of the systems. Factors like the placement of discharges within the cloud (strong dampening if in lower part) and type of hydrometeors surrounding the discharges (strong dampening in case of large hail and mixed phase hydrometeors) are complicating the interpretation. Therefore, this kind of product, based on GLM data, has become the least favoured by forecasters in the U.S. National Weather Service.

Chapter 4: Interpretation of LI data under different aspects

This chapter provides selected examples with preliminary insight into the interpretation of available LI (proxy) products.

Lightning jump

Sudden increases in the total lightning activity are seen as indication for an intensification of the thunderstorm and as a precursor of imminent severe weather (Williams, et al., 1999). Experience from the US shows that lightning jump signals can be expected from LI data but may be less distinct than seen at LMA data. Still, if lightning jumps become apparent in LI data, this can be considered as an indication for a sudden increase in severity if supported by other available data. (White, 2023)

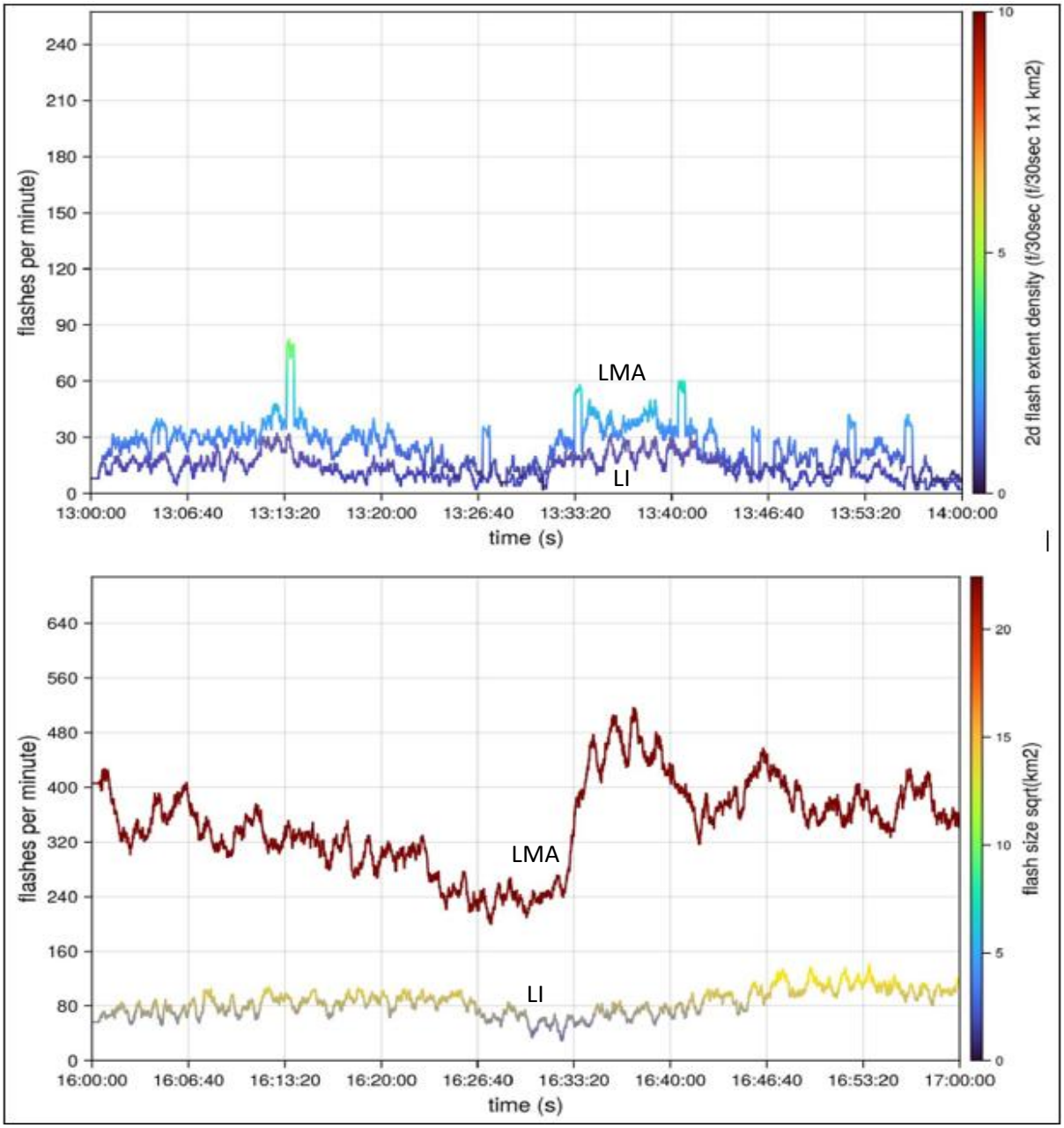

Fig. 4-1: Upper graph, example of low LMA flash rate on 31 October 2024: LI (darker colour) following the trend quite well. Lower graph, example of high LMA flash rate (wine red colour) on 2 August 2024: LI completely missing the most prominent lightning jump and being in general ill correlated. (van der Velde, 2024).

For LI data, no systematic studies are available yet but only few cases. For those few cases from the late 2024 convective season, the ability of LI to follow LMA trends was good for low flash rates, while for high LMA flash rates, i.e. with intense thunderstorms, such ability was lacking (see Fig. 4-1). Thus, it is currently not possible to provide clear LJ application guidance for forecasters.

Pulsing storms

Examples from weakly organized pulse storms in low shear environments show that LI can also detect infrequent flashes within such storms, even at high latitudes.

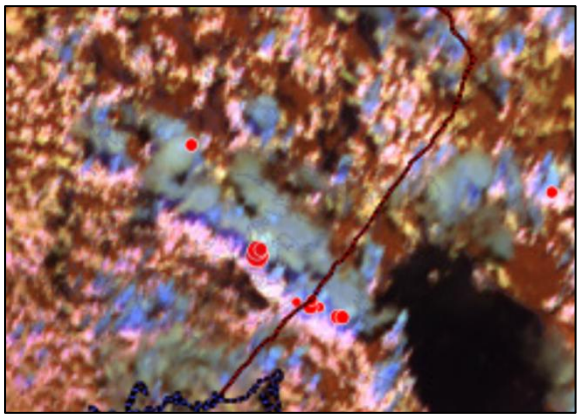

Fig. 4-2: Case of 12 August 2024, 12:20 UTC, SE Finland: FCI Cloud Phase with overlay of LI Flash Area (red dots of different size relative to the pixel size of the flash). No severe weather reported to the ESWD. A band of weak storms formed over southern Finland at 11 UTC. The band moved slowly southwest, producing isolated flashes in the stronger updrafts of the band. No major differences in the lightning activity were noted between the LI and the GLD360 system. Predominantly small flashes were detected in small convective cores with small anvils. Transient lightning activity was noted also in some single cells in the area. Combining the LI data with the Cloud Phase product reveals that flashes occurred especially with the updrafts that produced small ice crystals in their anvils (light blue colour in the RGB). Several cases from the 2024 convective season prove that LI is capable of detecting lightning at very high latitudes. Image source: EUMETSAT/ESSL, screenshot from ESSL Weather Data Displayer.

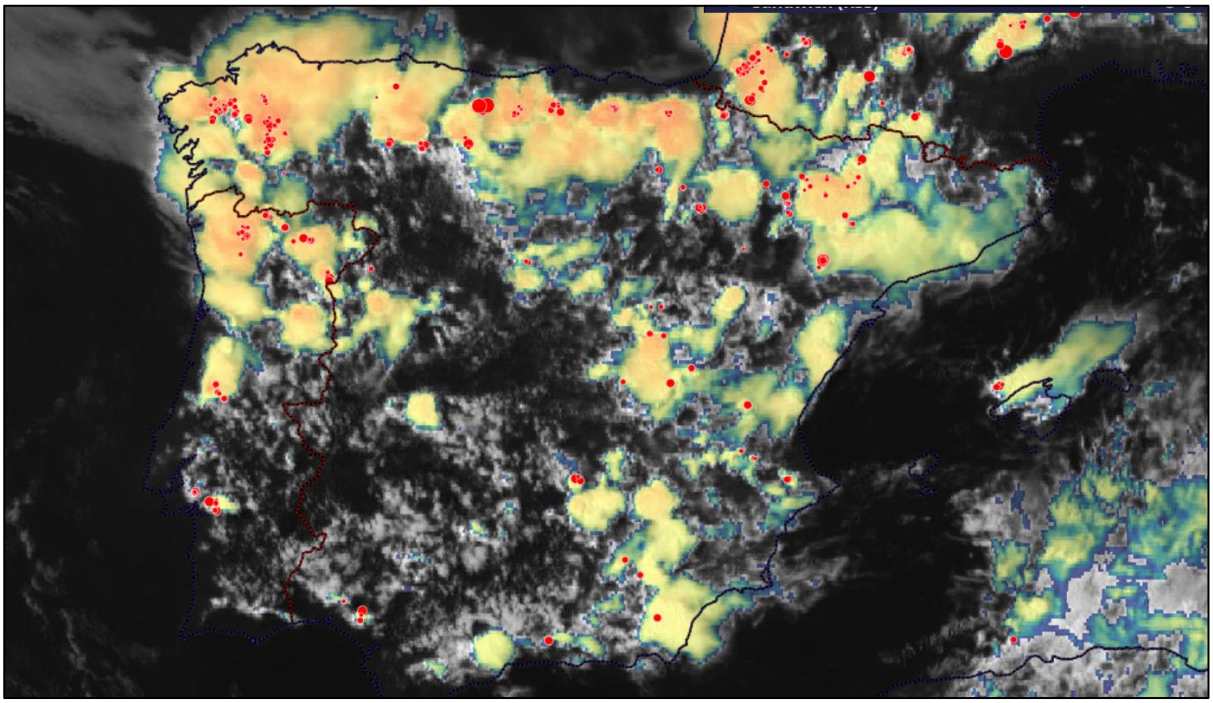

Fig. 4-3: Situation over Iberia with mostly unorganized convection at 15:00 UTC on 3 June 2023. Basic layer: Sandwich product. LI flash area point data potted on top. Red dots of different size: LI Flash area, 5-minute bin. The red dot radius is proportional to the logarithm of the flash area, which is given as a property of a flash. Image source: EUMETSAT/ESSL, screenshot from ESSL Weather Data Displayer.

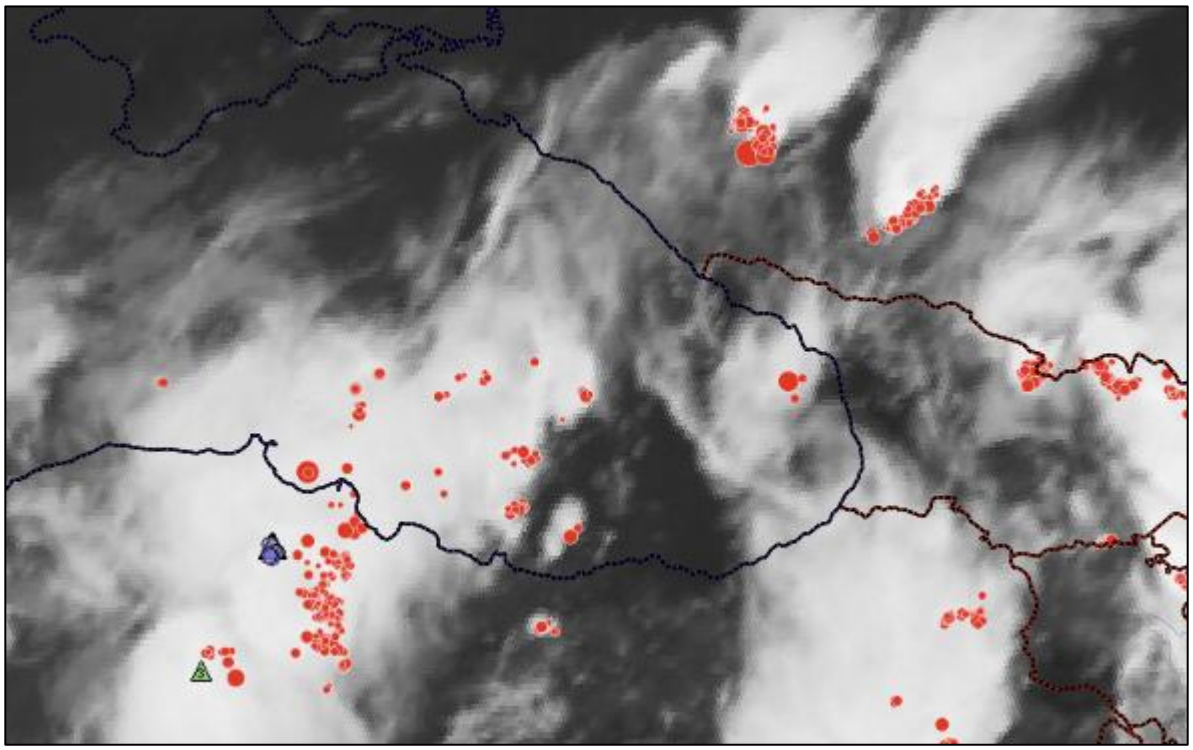

Fig. 4-4: Situation over the eastern Black Sea area at 16:25 UTC on 3 June 2023 with mostly non-severe thunderstorms. Basic layer: SEVIRI IR 10.8. Red dots of different size: LI flash area point data, 5-minute bin. The red dot radius is proportional to the logarithm of the flash area, which is given as a property of a flash. Green triangles: ESWD large hail events of past hour. Blue dots: ESWD heavy rain reports of past hour. Image source: EUMETSAT/ESSL, screenshot from ESSL Weather Data Displayer.

Severe storms

Knowledge on LI data interpretation in severe storms is limited at the time of publishing of this document. Only point data (LI Groups and LI Flashes) was available over larger fractions of the 2024 convective season. Preliminary findings from analysed cases suggest that …

- a high number of small, short-lasting flashes is an indication of the active (and strong) updraft areas in the convective complexes.
- very strong updrafts (capable of large hail) in supercells can result in a flash-free area surrounded by a ring of small-sized detections. This can be used as a marker in nowcasting.
- horizontally extensive flashes can be seen primarily in the trailing stratiform regions of large convective systems and can be taken as an indication of a still existing lightning strike threat, which involves potentially dangerous powerful positive CG strikes.

On the lightning rings or holes, Pucik & van der Velde (2024) discovered that LI point data is able to detect such features previously only known from LMA data.

Analysis of several cases hints that:

● LMA confirms these are indeed lightning holes.

● LMA shows more holes than are detected by LI.

● Not all LI holes may be LMA holes (more study needed).

● LI holes could offer an opportunity for severe weather detection by LI when flash rates essentially fail to detect jumps for more intense storms.

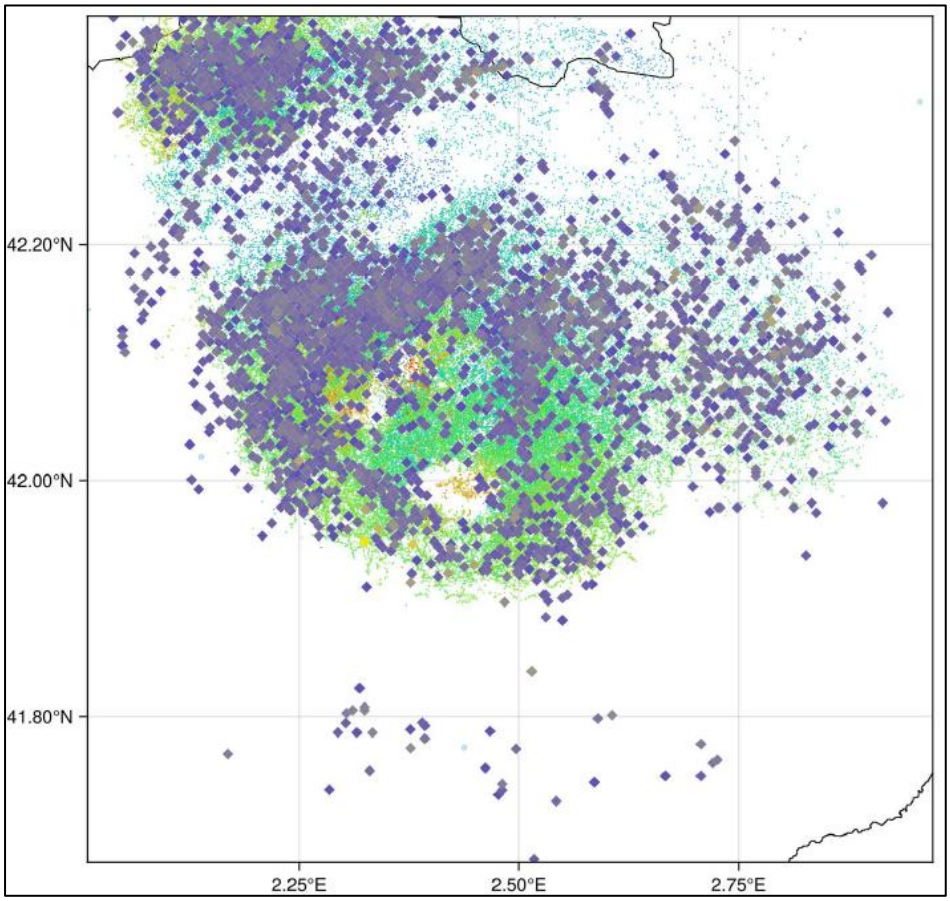

Fig. 4-5: A lightning hole detected by LMA (small dots) is largely reproduced by LI (large diamonds) for a case on 2 August 2024, 15:25:00 to 15:35:00 UTC. Source: van der Velde, personal communication.

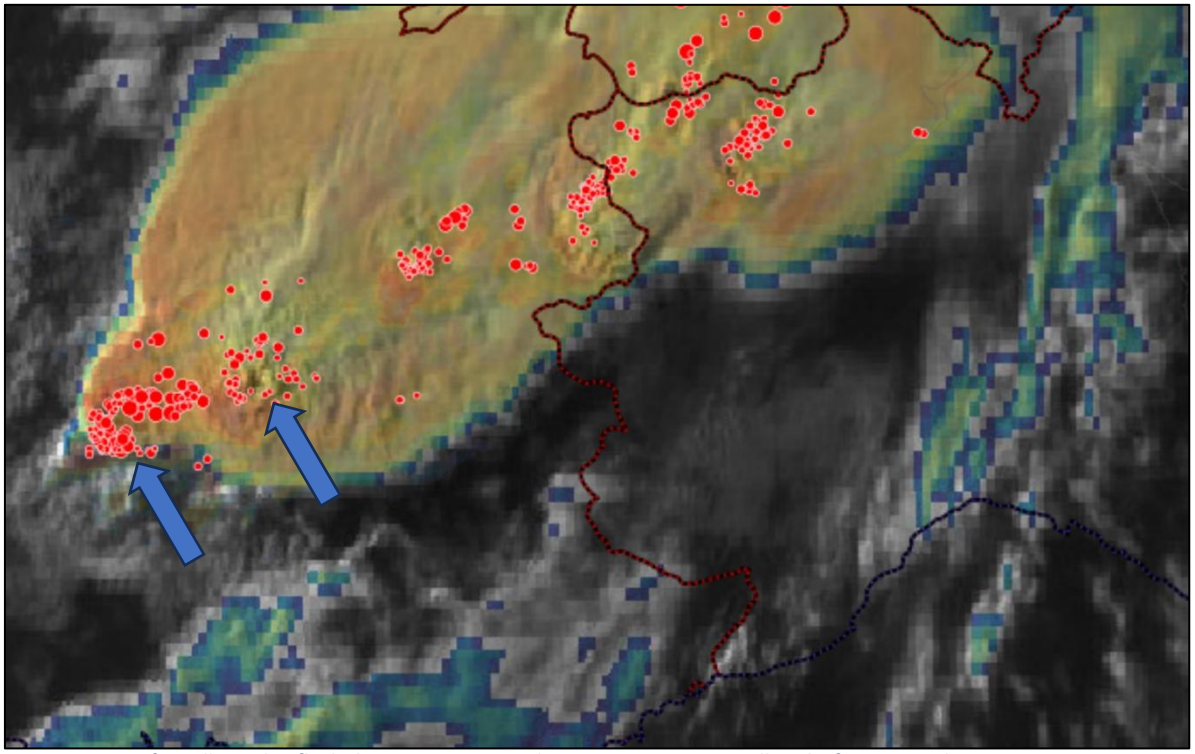

Fig. 4-6: Ring of small-sized LI flash detections surrounding an intense supercell updraft over southeastern France. Screenshot from ESSL Weather Data Displayer (source: EUMETSAT/ESSL). Red dots of different size: LI Flash area, 5-minute bin. The red dot radius is proportional to the logarithm of the flash area, which is given as a property of a flash. Overlay on SEVIRI Sandwich product. Image timestamp: 12 July 2023, 18:00 UTC.

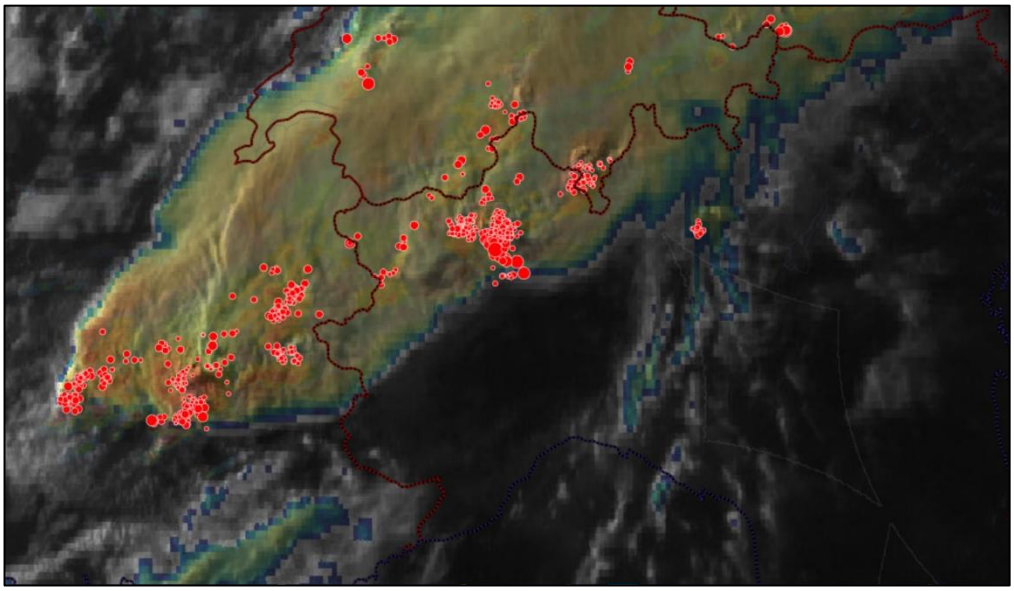

Fig. 4-7: Situation as of 12 July 2023, 18:35 UTC, with example of (not fully closed) lightning ring just under the overshooting top. Same image source and setup as for the previous figure.

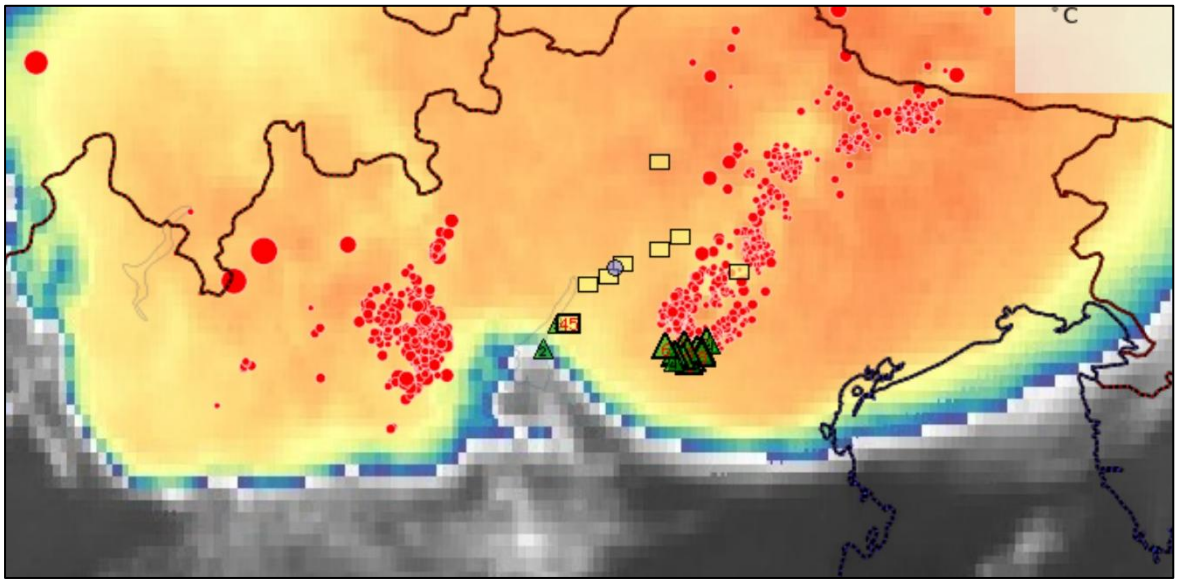

Fig. 4-8: Example of a lightning ring co-located (note parallax effect) with large hail (green triangles from ESWD data) over northeastern Italy at 22:55 UTC on 12 July 2023. Enhanced IR 10.8 from SEVIRI in background. LI Flash area display settings and image source as for previous figures.

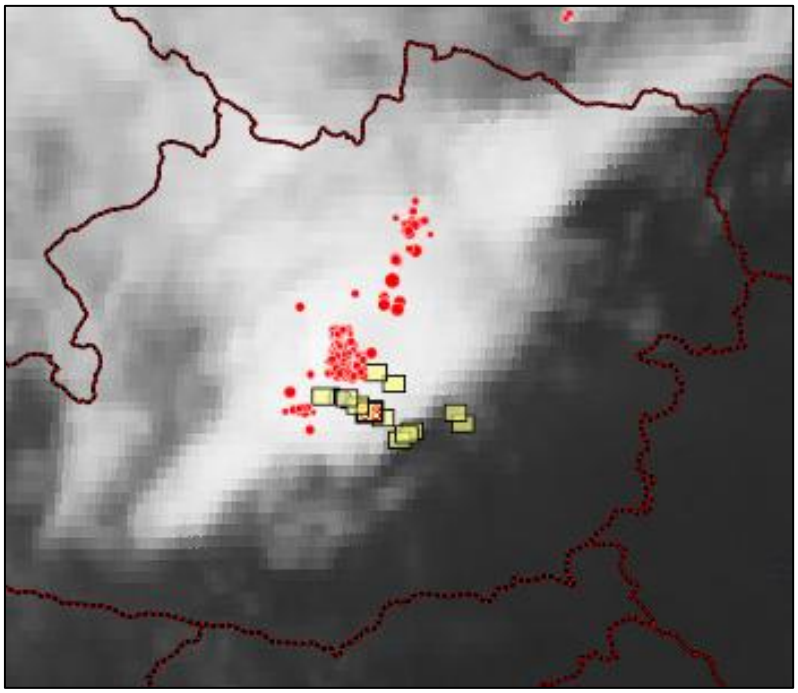

Fig. 4-9: LI flash area detections in connection with a severe convective wind event over central Austria. Red dots of different size: LI Flash area, 5-minute bin. The red dot radius is proportional to the logarithm of the flash area, which is given as a property of a flash. Overlay on SEVIRI IR 10.8. Image timestamp: 18:10 UTC on 12 July 2023. Yellow squares: ESWD damaging wind events plotted for the following hour. More lightning was detected during the formative and cellular stage of the system than during the later linear stage. The smallest flash sizes were detected where the most active updrafts were present. Screenshot from ESSL Weather Data Displayer (data sources: EUMETSAT, ESSL).

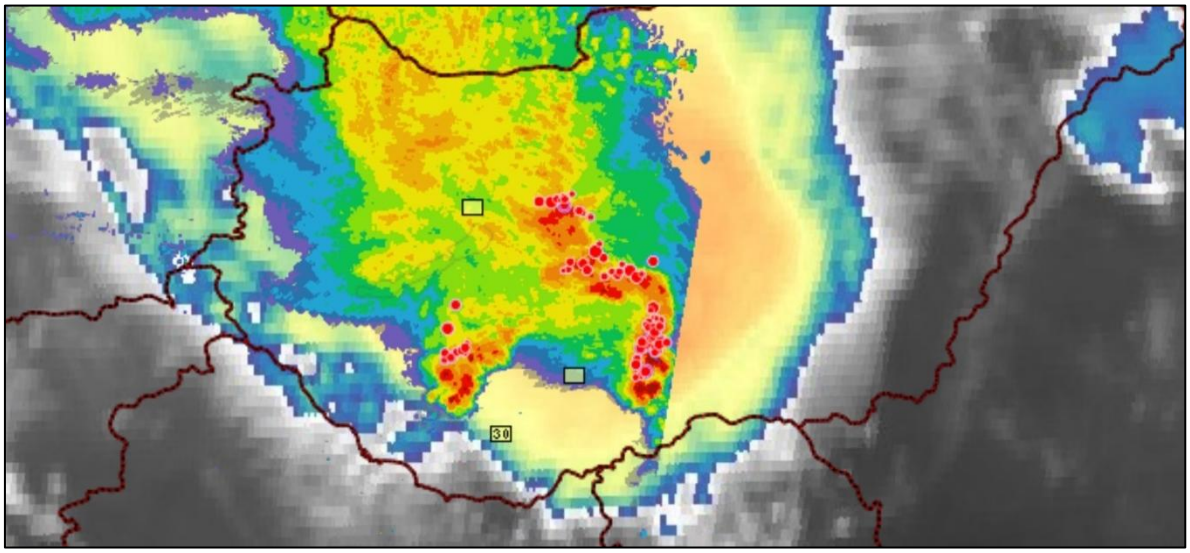

Fig. 4-10: Decaying bow-echo over Hungary at 04:45 UTC on 13 July 2023. LI Flash activity is decreasing. Overlay with enhanced SEVIRI IR and EUCOM radar composite in back layers. Top layer: ESWD hail (green triangles), severe wind gust reports (yellow boxes) of the previous 3 hours, and LI flash area (red dots). Flash area display settings and image source as for previous figure.

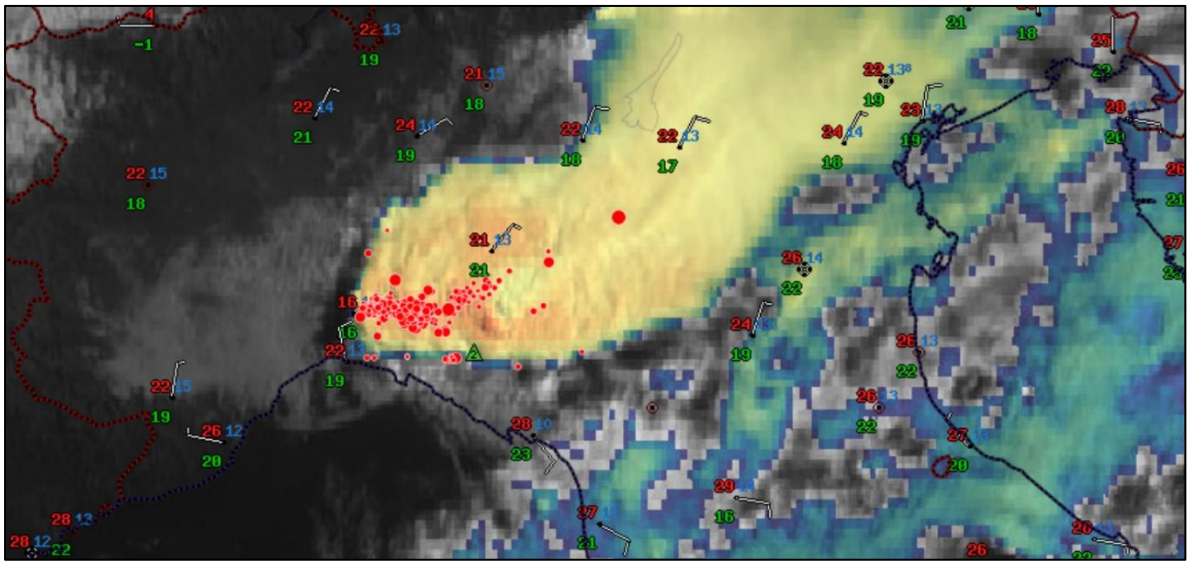

Fig. 4-11: Situation at 07:00 UTC on 13 July 2023 over northern Italy: single large flashes' optical signal emitted from the blowing-off anvil, mixed and medium-sized flashes in the western part of the storm, very small flashes next to the most prominent overshooting tops. Red dots of different size: LI Flash area, 5-minute bin. The red dot radius is proportional to the logarithm of the flash area, which is given as a property of a flash. Overlay on SEVIRI Sandwich product. Synoptic surface observations plotted for same time. Screenshot from ESSL Weather Data Displayer (sources: EUMETSAT, ESSL).

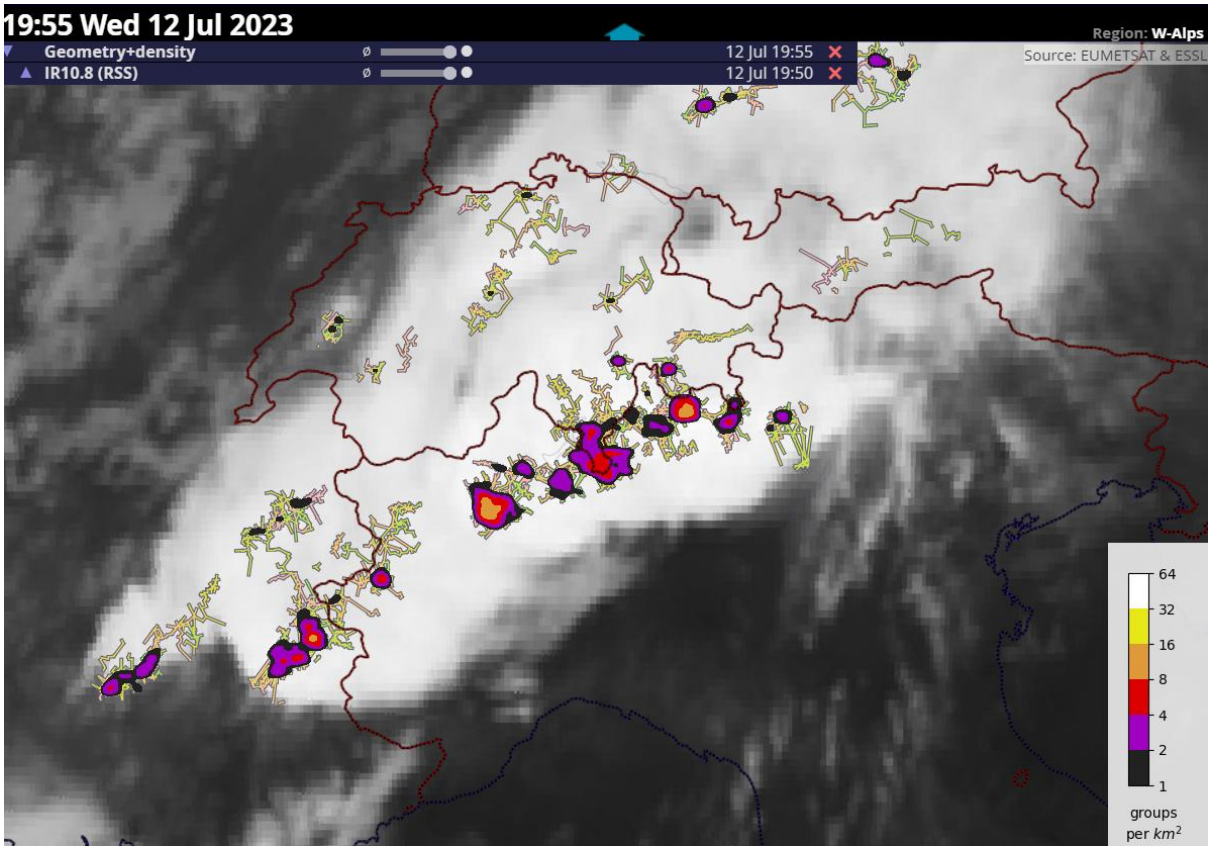

Fig. 4-12: Prototype example of ESSL combined lightning extent and density visualization. LI group data (point data) in 5-minute bin. Overlay of density of LI groups on a layer of flash geometry. Base layer: SEVIRI IR 10.8. Source data: EUMETSAT. Visualization: P. Groenemeijer/ESSL.

Chapter 5: Added value of MTG-LI products and summary of recent findings

LI data offers new prospects for nowcasting. LI Flash or LI Group size and density can be used for early identification of relevant processes that lead to intensification of thunderstorms and ultimately to severe weather events. While the identification of an elevated potential for heavy rain, convective wind events and tornadoes needs to be further examined, the potential for large hail warnings is already obvious based on early data analysis.

A range of new opportunities is evident for the use of gridded data in algorithms. NWC-SAF products and many other nowcasting products will be strongly backed by LI data that offers uniform data properties over large areas.

It was found very useful to work with LI point data both from the analysis but also nowcasting perspective.

LI group and flash point data inherits a downscaling effect (sub pixel grid resolution or pseudo-high resolution) that is based on physical properties (centroids on the basis of radiance weighting of pixel values / LI events) and not a pure procedural data manipulation effect. I.e. the radiance weighted centroids pick up brighter parts of the lit-up cloud. This effect helps to recognize features in severe storms that we know from LMA data too, for example flash holes in the overshooting top region. Due to the high optical thickness of clouds in the active updraft regions, anvil edges can become preferred zones for light emittance.

The baseline accumulated products are based on the event-level and appear to smooth or diffuse features, mainly as all lit-up event pixels are taken into account. This can include areas far away from the source of light, in extreme cases even large areas outside of the originating convective cloud system.

What we see from LI is a mix of lightning and cloud properties (dynamical, microphysical, and optical properties of the storm).

Comparison with LMA data revealed that, after applying geo referencing corrections individually per flash to account for parallax and other effects (linking of LI groups to the lightning channel as detected by LMA, shift of the whole flash based on the median of the deviations), LI group data mimics with striking similarity the geometry of lightning channels detected by the LMA sources. This was most obvious for positive leaders. Further studies are needed to confirm for larger samples.

While this can be taken as another indication that the interpretable spatial data resolution of LI centroids can be higher than the nominal pixel resolution of the LI instrument, this is especially the case for groups in the lower size spectrum but excluding those groups that are based on a very small number of underlying pixel events (1 or 2 only), as we are losing in those smallest cases the strength of the radiance-weighed centroids approach and merely reproduce the grid for the tiniest group sizes.

In addition, the following aspects were identified as added value relative to other data sources:

- Flash extent is a totally new type of lightning information (except for the very few regions with installed LMAs).
- High numbers of small flashes were found in the updraft areas of intense storms. This was especially true for the hailstorms.

- A ring of small flashes surrounding an overshooting top (or in general the updraft core), that is mostly free of LI detections, can be a sign for extraordinary strong convective updrafts with a high risk for large hail.
- A transition from small flashes in active updraft areas towards large flashes can be a sign of the decaying intensity of a convective cell.
- Very large flashes are mainly found in the stratiform regions of convective systems.
- Tracking total lightning activity of thunderstorms can be done in homogeneity across a large region in contrast to ground-based VHF lightning detection systems dependent on the density and distribution of sensors.
- CC flashes often precede CG strikes. We found the test LI data to be efficient in early CC flash detection.
- The geometric extent of flashes can be used as a minimum approximation for the areas currently being at risk of CG lightning strikes. Such information is otherwise only available from LMAs, but not from the common ground-based lightning detection networks.
- The geometric extent of flashes can be easily visualized and used for products for the general public. Additional public outreach products can, for example, include information on the largest flash-per-day.
- Gridded LI data can be used as input for advanced nowcasting products that combine different datasets.
- LI data refreshes more frequently than typical weather radar data.
- LI data offers opportunities for the identification of critical developments (and their underlying physical processes) that frequently lead to severe convective storm impacts, i.e. new physical insights into storm dynamics forecasters have never been able to use before.

For optimal exploitation, it is important to …

- carefully synchronize LI information with data from other sources.
- remember that raw LI data undergoes the parallax effect, as other imager data from satellites.
- check whether the used weather data display systems and workstations are ready to make use of the high refresh rates of LI data. US experience shows that a moving 5-minute time window, that is updated every minute, was optimal for their forecasters.

References

AMS. (2024). *American Meteorological Society*. Retrieved from AMS Lightning Glossary: https://glossary.ametsoc.org/wiki/Lightning

Bojinski, S. (2023). The Meteosat Third Generation Programme (MTG) – Lighting Imaging mission. *EUMETSAT-ESSL Workshop on GOES-GLM and MTG-LI*.

Brook, M., & Ogawa, T. (1977). The cloud discharge. In e. R. Golde, *Lightning vol. 1 - physics of lightning* (pp. 191 - 230). London: Academic Press.

Bruning, E. (2023). GLM and MTG LI accumulated product equivalencies and detection efficiency factors. *EUMETSAT-ESSL Workshop on GOES-GLM and MTG-LI*.

Bruning, E. C., & MacGorman, D. R. (2013). Theory and Observations of Controls on Lightning Flash Size Spectra. *Journal of the Atmospheric Sciences*.

Bruning, E. C., Tillier, C. E., Edgington, S. F., Rudlosky, S. D., Zajic, J., Gravelle, C., . . . … (2019). Meteorological Imagery for the Geostationary Lightning Mapper. *JRG Atmospheres*.

Brunner, K. N., & Bitzer, P. M. (2020). A First Look at Cloud Inhomogeneity and Its Effect on Lightning Optical Emission. *Geophysical Research Letters*.

Calhoun, K. M. (2023). GLM Experiments in the NOAA Hazardous Weather Testbed. *EUMETSAT-ESSL Workshop on GOES-GLM and MTG-LI*.

de Laat, J., Wentink, C., Wijnands, J., & Jacobs, A. (2023). Satellite lightning data applications at KNMI. *EUMETSAT-ESSL Workshop on GOES-GLM and MTG-LI*.

Defer, E. (2023). Personal communication.

Defer, E., Morvais, F., Prieur, S., Rimboud, A., Cornet, C., Krehbiel, P., & Rison, W. (2023). Concurrent Optical and Electromagnetic Observations of the Lightning Activity at Flash and Storm Scales. *EUMETSAT-ESSL Workshop on GOES-GLM and MTG-LI*.

Erdmann, F. (2020). *Préparation à l'utilisation des observations de l'imageur d'éclairs de Météosat Troisième Génération pour la prévision numérique à courte échéance (Preparation for the use of Meteosat Third Generation Lightning Imager obs. in short-term num. wea. predn.).* Toulouse, France: Ph.D. thesis, Université Toulouse 3 – Paul Sabatier. Retrieved from http://thesesups.ups-tlse.fr/4947/

Erdmann, F., & Poelman, D. (2023). GLM lightning measurements and their potential use for nowcasting. *EUMETSAT ESSL Workshop on GOES-GLM and MITG-LI*.

Erdmann, F., Defer, E., Caumont, O., Blakeslee, R. J., Pédeboy, S., & Coquillard, S. (2020). Concurrent satellite and ground-based lightning observations from the Optical Lightning Imaging Sensor (ISS-LIS), the low-frequency network Meteorage and the SAETTA Lightning Mapping Array (LMA) in the northwestern Mediterranean region. *Atmospheric Measurement Techniques 13*.

esa. (2023). *eoPortal*. Retrieved from https://www.eoportal.org/satellite-missions/meteosat-third-generation#li-lightning-imager

EUMETRAIN. (2020). *EUMETRAIN web site*. Retrieved from http://www.eumetrain.org/data/3/362/362.pdf

Fdez-Arroyabe, P., Kourtidis, K., Haldoupis, C., & al., e. (2021). Glossary on atmospheric electricity and its effects on biology. *Int J Biometeorol 65*, 5-29. doi:https://doi.org/10.1007/s00484-020-02013-9

Goodman, S. J., Blakeslee, R. J., Koshak, W. J., Mach, D., Bailey, J., Buechler, D., . . . Stano, G. (2013). The GOES-R Geostationary Lightning Mapper (GLM). *Atmospheric Research*.

Holzer, A. M. (2024). *Summary of the EUMETSAT-ESSL Expert Workshop on early MTG-LI L2 test data cases (train the trainers).* EUMETSAT-internal report.

Le Moal, S. (2023). Lightning data valorisation for forecasters, medias and NWP. *EUMETSAT-ESSL Workshop on GOES-GLM and MTG-LI*.

López, J. A., Pineda, N., Montanyà, J., van der Velde, O., Fabró, F., & Romero, D. (2017). Spatio-temporal dimension of lightning flashes based on three-dimensional Lightning. *Atmospheric Research 197*.

Montanayà, J., van der Velde, O., Pineda, N., & López, J. (2019). *ISS-LIS data analysis based on LMA networks in Europe.* EUMETSAT EUM/CO/18/4600002153/BV.

NOAA. (2021). *NOAA News & Features*. Retrieved from https://www.noaa.gov/stories/worlds-longest-lightning-flash-on-record-captured-by-noaa-satellites

NOAA. (2022). *NOAA Satellites Youtube channel*. Retrieved from https://www.youtube.com/watch?v=Zy2px2NYu_I

NOAA. (2023). *The Satellite Proving Ground at the Hazardous Weather Testbed*. Retrieved from http://goesrhwt.blogspot.com/

NWS. (2024). *NOAA NWS Lightning Glossary*. Retrieved from https://forecast.weather.gov/glossary.php?word=lightning

Peterson, M., Rudlosky, S., & Deierling, W. (2017). The evolution and structureof extreme optical lightningflashes. *Journal of Geophysical Research:Atmospheres,122*, 13,370–13,386. doi:https://doi.org/10.1002/2017JD026855

Pineda, N., Montanayà, J., van der Velde, O., & López, J. (2023). Evaluation of the Lightning Imaging Sensor (ISS-LIS) by means of VHF ground-based LLS, as a reference for the upcoming MTG-Lightning Imager. *EUMETSAT-ESSL Workshop on GOES-GLM and MTG-LI*.

Pohjola, H., & Grandell, J. (2016). *Meteosat Third Generation Lightning Imager: Flash and Accumulated products and test data for user readiness activities*. Retrieved from EUMETRAIN ELDW: https://resources.eumetrain.org/data/4/433/Session_6.pdf

Pucik, T., & van der Velde, O. (2024). Personal communication.

Rakov, V. A., & Uman, M. A. (2003). J- and K-processes. In *Lightning - Physics and Effects* (pp. 182 - 188). Cambridge University Press.

Rimboud, A., Farges, T., C.-Labonnote, L., Defer, E., Cornet, C., Thieuleux, F., & Dubuisson, P. (2022). Lightning Radiative Transfer in Thundercloud to Simulate Imaging and Photometric Observations. *AGU Fall Meeting AE33A-07.* Chicago.

Rudlosky, S. D., Goodman, S. J., Virts, K. S., & Bruning, E. C. (2018). Initial Geostationary Lightning Mapper Observations. *Geophysical Research Letters*.

Schultz, C. J., Allen, R. E., Murphy, K. M., Herzog, B. S., Weiss, S. A., & Ringhausen, J. S. (2021). Investigation of Cloud-to-Ground Flashes in the Non-Precipitating Stratiform Region of a

Mesoscale Convective System on 20 August 2019 and Implications for Decision Support Services. *Weather and Forecasting 36, 2*.

Stolzenburg, M., & Marshall, T. C. (2009). Charge structure and dynamics in thunderstorms. In *Lightning: Principles, Instruments and Applications - Review of Modern Lightning Research* (pp. 57-82). Springer.

Thiel, K., & Pym, H. (2022). *WHICH GLM COLOR SCALE IS BEST?* Retrieved from NOAA EWP BLOG Spring Experiments & Beyond: https://inside.nssl.noaa.gov/ewp/topic/glm/

van der Velde, O. (2024). *Personal communication*.

van der Velde, O. (2024). A large flash at the coast of Catalunya on 14 August 2024, 01:53:42 to 01:53:46 UTC. *Personal communication*.

Velde, O. A., & Montanyà, J. (2013). Asymmetries in bidirectional leader development of lightning flashes. *Geophys. Res. Atmos.*, 118, 13,504–13,519. doi:10.1002/2013JD020257

Viticchiè, B. (2020). *MTG LI System Commissioning: LI lightning detectin performances – based on the presentations from the LI MAG meeting #8*. Retrieved from EUMETSAT CDN: https://www-cdn.eumetsat.int/files/2020-05/pdf_mtg_li_mag_9_perf_assess.pdf

White, K. (2023). Experiences with Total Lightning Data and Experimental GLM-based Products in the Operational Environment. *EUMETSAT-ESSL Workshop on GOES-GLM and MTG-LI*.

Williams, E., Boldi, B., Matlin, A., Weber, M., Hodanish, S., Sharp, D., . . . Buechler, D. (1999). The behavior of total lightning activity in severe. *Atmospheric Research 51*.

Zhang, D., & Cummins, K. L. (2020). Time Evolution of Satellite-Based Optical Properties in Lightning Flashes, and its Impact on GLM Flash Detection. *JGR Atmospheres*.

Addendum

This document is based on content from a series of expert workshops, the most recent one in November 2024. We are deeply grateful to the authors of the workshop talks for allowing us to use some of their content for this guide.

The list of contributors in alphabetical order:

Stephan Bojinski (EUMETSAT, Germany), Eric Bruning (TTU, USA), Kristin Calhoun (NOAA, USA), Michaël Claudon (MeteoFrance, France), Sven-Erik Enno (EUMETSAT, Estonia), Felix Erdmann (Meteo BE, Belgium), Eric Defer (CNRS, France), Pieter Groenemeijer (ESSL, The Netherlands), Jean-Babtiste Hernandez (MeteoFrance, France) Ty Higginbotham (NOAA, USA), Gerrit Holl (DWD, Germany), Alois M. Holzer (ESSL, Austria), Ronan Houel (MeteoFrance, France), Zsofia Kocsis (HungaroMet, Hungary), Laura Kuzmenko (LVGMC, Latvia), Jos de Laat (KNMI, The Netherlands), Alessandro Marraccini (IPMA, Portugal), Sylvain Le Moal (Meteo France, France), Jean-Marc Moisselin (MeteoFrance, France), Joan Montanya (UPC, Spain), Nicolau Pineda (Meteocat, Spain), Tomas Pucik (ESSL, Slovakia), Benjamin Rösner (DWD, Germany), Wolfgang Schulz (ALDIS, Austria), Ivan Smiljanic (EUMETSAT, Croatia), Natasa Strelec Mahovic (EUMETSAT, Croatia), Oscar van der Velde (UPC, Spain), Kris White (NOAA, USA), Bartolomeo Viticchie (EUMETSAT, Italy), Andreas Wirth (GeoSphere Austria, Austria).

Figure 0-1: Participants at the Expert Workshop on GOES-GLM and MTG-LI in early spring 2023 (photo: Alois M. Holzer)

This document was first presented in a provisional version (“Proto Short Guide”) and was iterated after the first full convective season with METEOSAT Third Generation Lightning Imager (MTG LI) data from summer 2024. Feedback from ESSL-EUMETSAT Forecaster Testbeds was taken into account.

This application guide is focussed on the needs of forecasters and is complementary to the LI L2 Product User Guide (PUG) that can be found on the EUMETSAT User Portal:

https://user.eumetsat.int/resources/user-guides/mtg-li-level-2-data-guide

Figure 0-2: Participants at the second MTG-LI Expert Workshop in early spring 2024 (photo: EUMETSAT)

Notes: